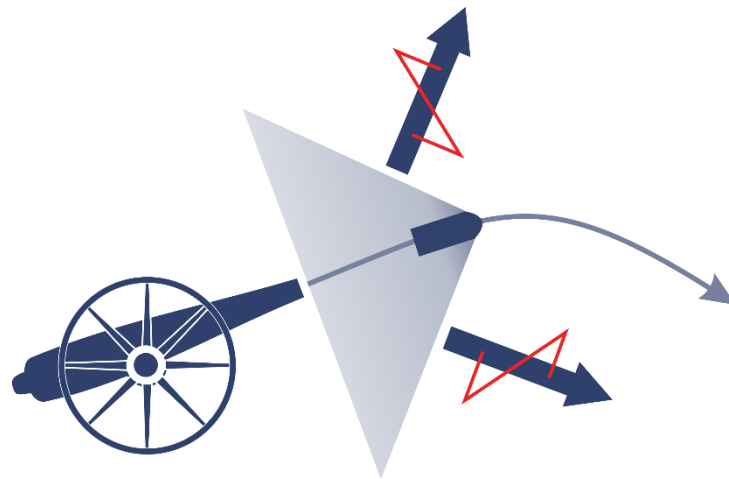


Projectile Sound

To Whom It May Concern



Kennung: kwhdba.08.02
Datum: 22.08.2018
Status: Entwurf

Content

1	Introduction	3
1.1	The challenge	3
1.2	The relevant Part 2 and Part 4 of the EN ISO 17201 series.....	3
1.3	Widening the Scope	4
2	Source energy estimation.....	5
2.1	The generation of projectile sound	5
2.2	Estimation of the source energy of the projectile sound.....	7
2.3	A typical trajectory	8
3	Geometric spreading.....	9
3.1	What is geometrical spreading.....	9
3.2	The cylindrical approach.....	9
3.3	The geometric spreading of a trajectory segment.	9
4	Sound exposure.....	12
5	The Signal of projectile sound.....	13
5.1	Non-linear effects.....	13
5.2	The N-wave.....	14
5.3	The exposition of an N-wave	15
5.4	Estimation of the characteristic time duration	15
5.5	Estimation of the characteristic pressure	16
6	Technical model to predict sound levels	19
6.1	The need of a technical model	19
6.2	Concept for a general linear model for projectile sound.....	19
6.3	On how to estimate a limit of linearity	20
7	Discussion.....	22
7.1	The relevant parameters of a projectile.....	22
7.2	The MACH number	22
7.3	Resumé.....	25
8	Example.....	27
8.1	Howitzer.....	27
8.2	Close up pressure time histories of the projectile sound of a 5.56 shot.....	32
9	Conclusion.....	41
10	References	42
11	Appendix	43
11.1	Remark on Eq. 28	43
11.2	Drag coefficient	44
11.3	Trajectory.....	45
12	Über „Bella Acustica – De Bello Acustico“	46

1 Introduction

1.1 The challenge

In general, any solid body radiates the so-called projectile sound (or sonic boom) if it moves through the air at rest with a speed higher than the local sound speed. This essay focus on rather simple bodies of revolution following a path that is called the trajectory. The body will fly along a ballistic trajectory if it is not propelled or along a more general curve if it is propelled like a rocket for instance.

Fundamental research was done by WITHAM in 1952, see []. PIERCE uses in his book [] the results of WITHAM to formulate a (sound)pressure-based scheme to predict the sound pressure in the vicinity of the projectile if the trajectory is a straight line and the projectile speed reduces linearly along its trajectory. This scheme considers the non-linear sound propagation effects.

1.2 The relevant Part 2 and Part 4 of the EN ISO 17201 series

The projectile sound model of EN ISO 17201-4 relies on the scheme of WHITHAM and PIERCE mentioned above. This model predicts the sound pressure of the projectile sound at an arbitrary receiver point considering the dimensions of the projectile and its linearly decaying speed along its straight trajectory.

EN ISO 17201-2 provides guidance on how to estimate source parameters for the relevant sounds that occur while the shooting a weapon or firing explosives. The relevant shooting sounds are the muzzle blast and the projectile sound. The basic idea of part 2 is to use the energy that is involved in both cases to estimate the acoustical source energy of the sound under consideration. However, having the energy is not sufficient to describe the acoustics of the source. In addition to the energy, information on spectrum and is needed in order to setup a source model. Hence, Part 2 also supplies for each the two cases a model that allows to assign a spectrum to the source energy.

Note

We will neglect the directionality here.

For the muzzle blast it is the energy of the propellant or the energy of the explosives used respectively. Assuming that the fraction of energy that converts to acoustical energy is constant, the acoustical source energy is simply proportional to the total energy. The ‘signal-model’ is the Weber-model that gives the spectrum depending on the acoustical source energy.

For the projectile noise it is the kinetic energy loss of the projectile along a trajectory segment of unit length due to air friction. The ‘signal-model’ is – if you like – the pressure model in Part 4 with some modifications.

1.3 Widening the Scope

Though the scope of the EN ISO 17201 series restricts its application to so-called small arms (caliber smaller than 20 mm or TNT-equivalent demolitions less the 50 g) the concepts of part 2 are ready to be applied to weapons with larger caliber and high explosions. Historically, this restriction was introduced during the definition of the working item through the standardization boards that initiated the standard. In the 1990, when the Joint Working Group 51 started to draft the first parts of the series the main title was “*Acoustics — Noise from shooting ranges*”. Nevertheless, the procedures in the standard, in particular Part 1, Part 2 and Part 4, were developed and validated in the context of military shooting.

If you are looking for specific features for large weapons refer to ISO 13474 "Acoustics – Impulse sound propagation for environmental noise assessment".

2 Source energy estimation

2.1 The generation of projectile sound

Even a simple view on projectile sound its generation and its propagation is not really 'simple'. It is not just modelled as a point source with clear geometric spreading having a source energy and a spectrum (and a possible directivity).

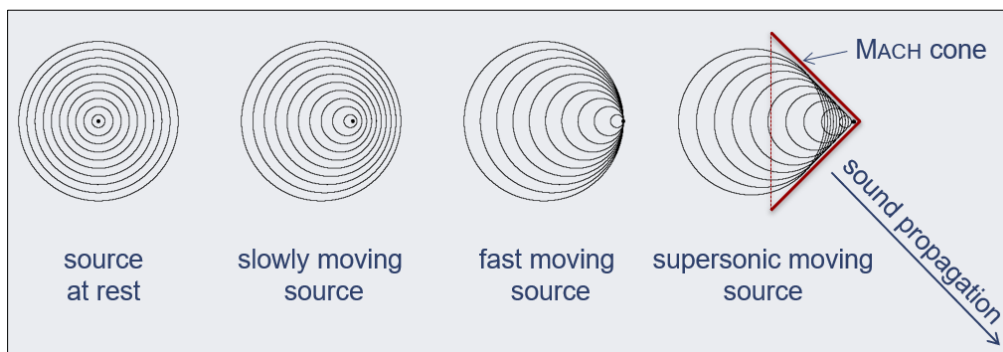


Figure 1 The generation of projectile sound due to superimposing spherical waves

In textbooks sonic boom is normally introduced as an interference phenomenon of spherical waves of a source at supersonic speed. Figure 1 indicates this idea. Obviously, a shock front generates as a straight line or cone – the so-called MACH cone - if rotated around the flight path of the source.

For a projectile generating projectile sound this idea is not applicable. The source in Figure 1 also radiates sound if it is at rest. The energy of the shock seems to stem from the power of the source. Projectiles are no sound sources; if they lie on a table they are quiet 😊. Therefore, projectile sound must take the acoustical energy out of the kinetic energy of the projectile somehow. If the projectile is not propelled, its velocity will necessarily have to change along the path. Figure 1 also presumes that the source is moving on straight line. A projectile, however, normally will face gravity which will introduce ballistic flight paths if it is not propelled. Finally, not only the energy will be reduced along the flight path but also the momentum. Hence, the idea of Figure 1 is not applicable to projectile sound.

Projectile sound is radiated from everywhere along the trajectory of the supersonic moving projectile.

Note

'Trajectory' is the more appropriate wording for the flight path of a projectile.

Normally, trajectories are by no means a straight line. They ballistic curves in case of unpropelled projectiles and they can be of any shape if they are propelled as a rocket for instance is. Figure 2 shows a sketch that is more realistic though the drawing of the MACH cone there is rather wrong. The shock front never forms a cone around a ballistic trajectory due to the change of speed and direction of the projectile. The MACH cone in Figure 2 is only meant to indicate the angles that are relevant to describe the local radiation.

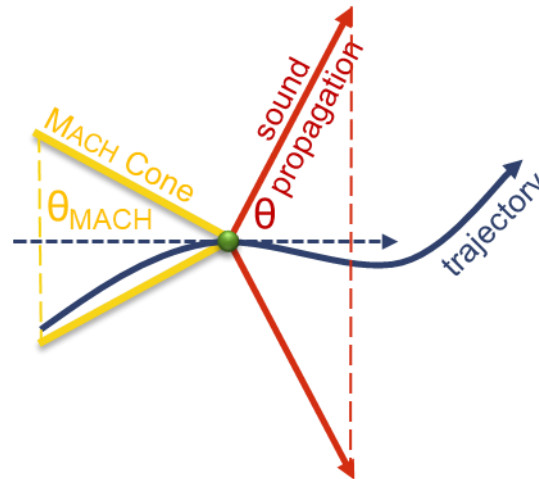


Figure 2 Principal sketch of relevant directions (Mach cone yellow, sound propagation direction red for the radiation of projectile sound at a position P (green) at the trajectory (blue); the dashed blue line indicates the direction of the trajectory at P.

At a projectile position P on the trajectory (solid blue line in Figure 2) sound is radiated only into a cone (red arrows). The yellow lines indicate so-called MACH cone that would develop as location of the shock front if the project flies along the dashed line with constant speed. The axis of revolution of the cones is the axis of revolution of the projectile at position P. The opening angle the so-called MACH angle θ_{Mach}

$$\theta_{Mach} = \arcsin\left(\frac{1}{M}\right) \quad \text{Eq. 1}$$

Note

The MACH angle does not indicate the direction of sound radiation. The sound is always radiated perpendicular to the surface of the MACH cone.

The angle of sound propagation relative to local tangent to the trajectory is given in Eq. 2.

$$\theta = \arccos\left(\frac{1}{M}\right) \quad \text{Eq. 2}$$

2.2 Estimation of the source energy of the projectile sound

It is clear, that the acoustical energy of the projectile sound must be a fraction of the energy loss of the projectile. Hence, the first goal is to estimate the energy loss of the projectile along its trajectory. This energy loss is due to air friction.

Let us assume that the trajectory is divided in straight segments of a certain length and let us denote each segment through the index i for later use.

We further assume that

- the projectile velocity is parallel to the segment
- the Mach number M of the projectile varies only linearly along the segment
- the drag coefficient C_w of the projectile which depends on M varies only linearly along the segment
- the air density ρ is constant
- the speed of sound c is constant
- the cross-section A of the projectile is constant

Then, the projectile energy loss can be calculated as the line-integral of the drag-force along the trajectory from $P_{b,i}$ to $P_{e,i}$ the beginning and end point of the segment. Let denote s_i the length of the segment.

Considering the constraints on the segment properties given above the following formulae can be derived as sufficiently precise approximations of the line integral over the drag force for the segment i , see [1], [2]. The formulae yield the energy loss of the projectile, not the resulting acoustical energy of the sound radiated from the segment.

$$Q_i = \frac{s_i}{2} \rho A c^2 \frac{1}{M_{b,i} - M_{e,i}} \left\{ \begin{array}{l} \frac{1}{3} (M_{e,i}^2 + M_{b,i} M_{e,i} + M_{b,i}^2) (C_{wb,i} M_{e,i} - C_{we,i} M_{b,i}) + \dots \\ \dots + \frac{1}{4} (M_{e,i}^3 + M_{e,i}^2 M_{b,i} + M_{e,i} M_{b,i}^2 + M_{b,i}^3) (C_{wb,i} - C_{we,i}) \end{array} \right\} \quad \text{Eq. 3}$$

Eq. 3 applies to the most general case under the given constraints. Both, M and C_w are different at $P_{b,i}$ and at $P_{e,i}$.

$$Q_i = \frac{s_i}{6} \rho A c^2 C_{w,i} (M_{e,i}^2 + M_{b,i} M_{e,i} + M_{b,i}^2) \quad \text{Eq. 4}$$

Eq. 4 holds in such cases where it can be assumed that the drag-coefficient does not change from $P_{b,i}$ to $P_{e,i}$

$$Q_i = \frac{s_i}{2} \rho A c^2 C_{w,i} M_i^2 \quad \text{Eq. 5}$$

Eq. 5 is the result for the cases where the drag-coefficient and the projectile speed can be assumed to not change along the segment.

Which formula to use basically depends on the change of the drag-coefficient which is a function of the speed itself. In order to get some idea about the dependency of the drag-coefficient on the speed, we will have a look into an example.

Q_i provides the energy loss of the projectile along the segment i . A fraction $\sigma_{ac,i}$ of this energy will be the acoustical source energy $Q_{ac,i}$ of the projectile sound, see Eq. 6. This fraction may depend on the speed of the projectile and on its shape.

$$Q_{ac,i} = \sigma_{ac,i} Q_i \quad \text{Eq. 6}$$

2.3 A typical trajectory

The following figures shows the features of a typical rifle shot taken from [3]. The drag-coefficient in Figure 32 indicates the typical shape of this parameter that holds for the most of projectiles, even for howitzer shells for instance.

Note

In English literature c_d denotes the drag-coefficient instead of C_w in German literature (Widerstandsbeiwert)

The massive change of the drag-coefficient with close to the speed of sound highlights that the wording ‘sonic wall’ has some nuggets of truth in it. Approaching from subsonic speed there is a strongly increasing resistance for any object to be accelerated beyond the sound speed. If that wall is torn down its getting more and more easier to arrive at higher speeds.

Note

The appendix (chapter 11.2 and 11.3) present some figures which may help the reader to get some ideas of the basic quantities of a shot.

3 Geometric spreading

3.1 What is geometrical spreading

Geometrical spreading means different things in different context. From a principal point of view, a point source radiates its source strength (energy or power depending whether the source describes a single event or a continuous signal) through spheres around the source. Therefore the source strength spreads over the surface of the sphere, and because the surface area of the sphere increase with the square of its radius r the geometric spreading of a point source is said to be $\frac{1}{r^2}$. For line sources it is obvious that the spheres are to be substituted by cylinders of radius r and yield a geometric spreading of $\frac{1}{r}$. This is a source-related view on geometric spreading because this definition does not include any propagation features.

There is different view that only considers the propagation. Let us assume sound energy is spread over a certain area A_b . After some propagation the same energy may be spread over an area A_e . The geometric spreading is then defined as the ratio of both areas.

As an example, let us put a point source in a tube and let it radiate a blast. At a distance smaller than the diameter of the tube the spreading will be spherical. At distances much larger then diameter there is no geometric spreading anymore ($A_b = A_e = const$). The geometric spreading of that source depends on the distance and the tube diameter: it is not spherical as it is stated for a point source.

We will see that even the source-related geometric spreading of projectile sound is neither cylindrical nor spherical.

3.2 The cylindrical approach

Considering the view on sonic boom according to Figure 1, it is clear that related areas are cones with constant opening angle. The surface of these cones grows with distance from the flight path. Hence, the geometric spreading of this model is proportional to $\frac{1}{r}$ which means cylindrical. However, this model is not applicable to projectile sound.

3.3 The geometric spreading of a trajectory segment.

In general, the projectile speed at the begin at the end of a trajectory segment i of finite length is not the same. The angle of sound propagation is different according to Eq. 2. We need to

arrange some definitions on geometric parameters to formulate an estimation for the geometric spreading of the projectile sound.

Let denote P_s the reference source point of the projectile sound from the segment. This is the endpoint of segment. Let denote θ_b and θ_e the sound propagation angle at the starting point and the endpoint of the segment.

Any receiver point that will in the region between these two angles will get projectile sound from the segment. In three dimension this is the volume between the two cones that belong to the both angles. For the estimation of the relevant area the energy of the source is spread over in a given distance r it is mandatory that the sound penetrates the area parallel to the area vector. Therefore, we choose the relevant receiver point along the straight line starting in P_0 at the direction of θ_b and consider the area orthogonal to this line. Figure 3 sketches the situation and indicates the meaning of the parameters.

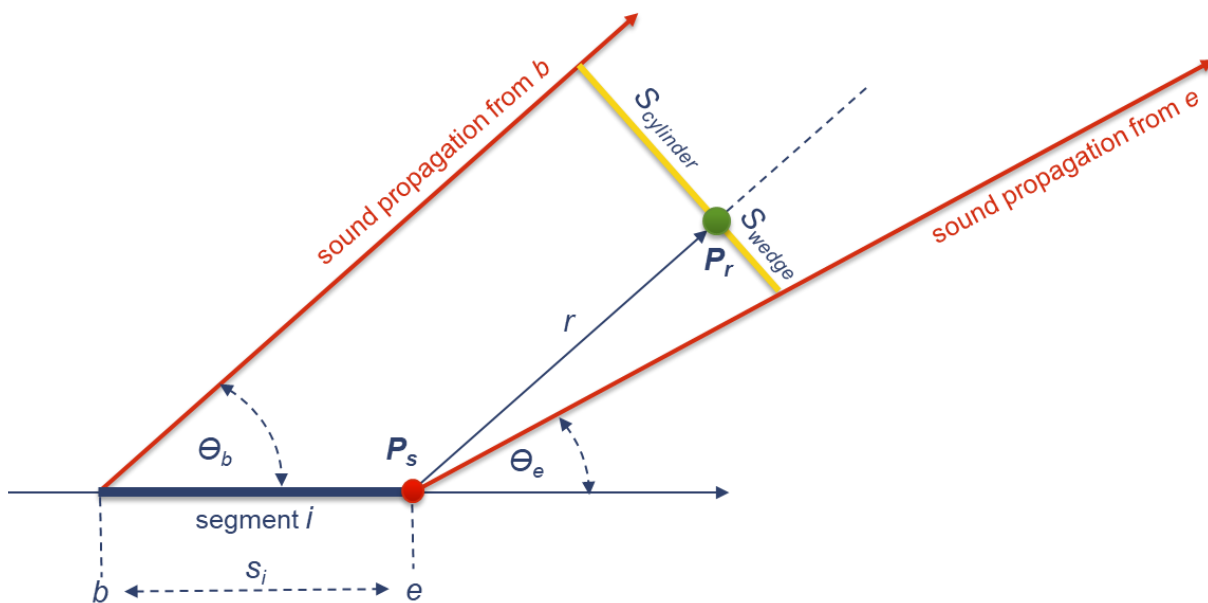


Figure 3 Geometry for the calculation of geometric spreading

Obviously, the relevant area S_i has two parts, a cylindrical one $S_{cylinder,i}$ and wedge $S_{wedge,i}$.

$$S_i = S_{cylinder,i} + S_{wedge,i} \tag{Eq. 7}$$

After some geometric calculations these areas can be expressed through parameters that only depend the trajectory.

$$S_{cylinder,i}(r) = 2 \pi s_i \sin^2(\theta_{b,i}) \left(\frac{1}{2} s_i \cos(\theta_{b,i}) + r \right) \quad \text{Eq. 8}$$

$$S_{wedge,i}(r) = 2 \pi r^2 \sin\left(\theta_{b,i} - \frac{\theta_{e,i} - \theta_{b,i}}{2}\right) \sin(\theta_{e,i} - \theta_{b,i}) \quad \text{Eq. 9}$$

The cylindrical area in Eq. 8 has a part that is independent from the distance and a part that increases with distance. The cylindrical part indicates a geometric spreading of $1/r$ and the distance dependent part is proportional to the length of the segment indicated that the source is a line source somehow. Eq. 9 indicates a wedge introduces a spherical spreading $1/r^2$ because the area increases with the square of the distance. And it does not depend on the length of the segment. Obviously, this is the spreading of a point source.

As a conclusion, the source of the projectile sound looks like a combination of a point source and a line source, so far geometric spreading is concerned. The cylindrical source will lose importance if θ is small. Hence, if the projectile speed is close to speed of sound (θ tends to 0) the geometric spreading of the projectile sound is spherical.

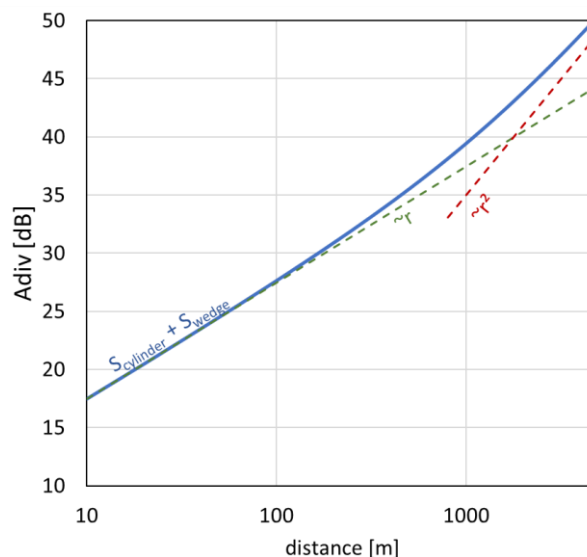


Figure 4 Example of a typical geometrical spreading of the projectile sound. Example is taken from the .223 Remington shot discussed later in this paper

Figure 4 indicates the geometrical spreading and compares it to pure cylindrical and spherical spreading. In this case of a fast projectile on a straight trajectory the transition from cylindrical to spherical spreading is already relevant at a distance of about 300 m.

4 Sound exposure

This chapter assumes that the trajectory is ‘simple’ in such a way that there is only one segment i that contributes to the noise load in a receiver point P_r .

Note

Trajectories of rockets for example need not to match this condition because there are accelerated before they follow a ballistic flight path. Then, receiver point in particular region may receive projectile sound from more than one segment

A certain fraction of the source energy determined

Furthermore, we will neglect any other phenomena of sound propagation than geometric spreading. Then, the pressure exposure E_p at the receiver point is given as the source energy (of the single event projectile sound) time the impedance of air divided by the area the sound is penetrating.

$$E_{p,i}(P_r) = \rho c \frac{Q_{ac,i}}{S_i} \quad \text{Eq. 10}$$

Using Eq. 3 for the energy and Eq. 8 including Eq. 9 and Eq. 9 for the geometric spreading yield

$$E_{p,i}(P_r) = \frac{\frac{s_i \rho^2 A c^3 \sigma_{ac,i}}{2(M_{b,i} - M_{e,i})} \left\{ \begin{array}{l} \frac{1}{3}(M_{e,i}^2 + M_{b,i}M_{e,i} + M_{b,i}^2)(C_{Wb,i}M_{e,i} - C_{We,i}M_{b,i}) + \dots \\ \dots + \frac{1}{4}(M_{e,i}^3 + M_{e,i}^2M_{b,i} + M_{e,i}M_{b,i}^2 + M_{b,i}^3)(C_{Wb,i} - C_{We,i}) \end{array} \right\}}{2\pi \left[s_i \sin^2(\theta_{b,i}) \left(\frac{1}{2}s_i \cos(\theta_{b,i}) + r \right) + r^2 \sin\left(\theta_{b,i} - \frac{\theta_{e,i} - \theta_{b,i}}{2}\right) \sin(\theta_{e,i} - \theta_{b,i}) \right]} \quad \text{Eq. 11}$$

This is a rather lengthy formula. A reasonable simplification is not possible though it can be given in other views.

5 The Signal of projectile sound

5.1 Non-linear effects

It is well-known that projectile sound forms a typical N-wave, a basically rather simple time history of the pressure. The signal does not exist at the source that means direct at the projectile. It develops as such due to non-linear effects.

Acoustic in gases is in principal non-linear. Linear acoustics applies if the sound pressure and the particle velocity of a plane wave is governed by a linear equation. In gases however, even in an ideal gas, the volume change does not yield a proportional pressure change. The basic law is a hyperbolic function. The linear approach needs to approximate the hyperbolic function through a straight line. This approach gets better if the volume change is smaller, see Figure 5.

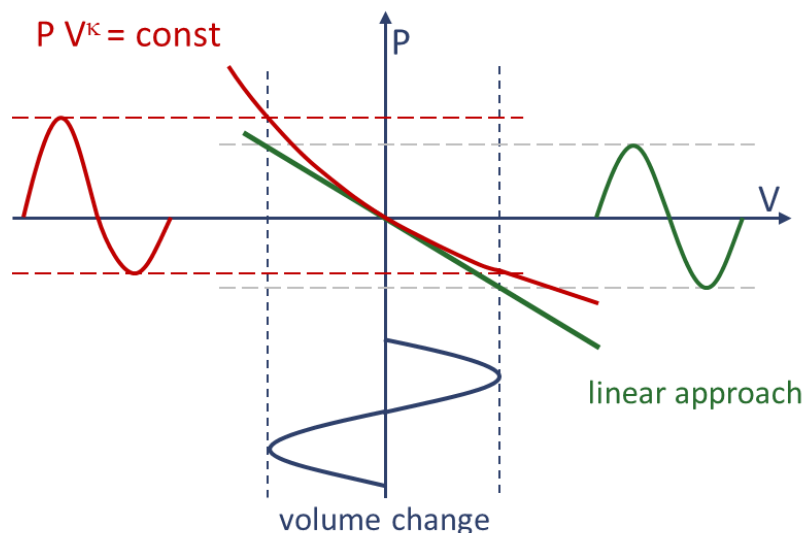


Figure 5 Sketch to indicate non-linear distortion of an acoustic signal in an ideal gas; let P denote the pressure and let V denote the volume

In addition, the speed of sound increases if the pressure increases. That means the high positive pressure part of the signal travels faster than its negative companion. A sinus wave will be distorted to an N-wave. Figure 8 drafts this effect under the assumption that the sound exposure is const.

Note

There are more non-linear effects. For instance, the sound wave needs to carry momentum that the projectile loses along its trajectory. Therefore, the positive part of the signal is larger and has a dc-component in the pressure, the so-called radiation pressure which generates a dc air flow.

Projectile sound from a real projectile is much more complex. The friction will for instance heat up the air in the direct vicinity of the body changing impedance and the speed of sound there

for instance. Directly behind the projectile turbulences destroys the airflow and a clear acoustics by any means. Hence, all following statements a more a less approaches to reality.

In addition, every change in the projectile's diameter will generate its own shock wave. Due to the non-linear effects the merge together – they are not superimposing - to finally form a simple N-wave.

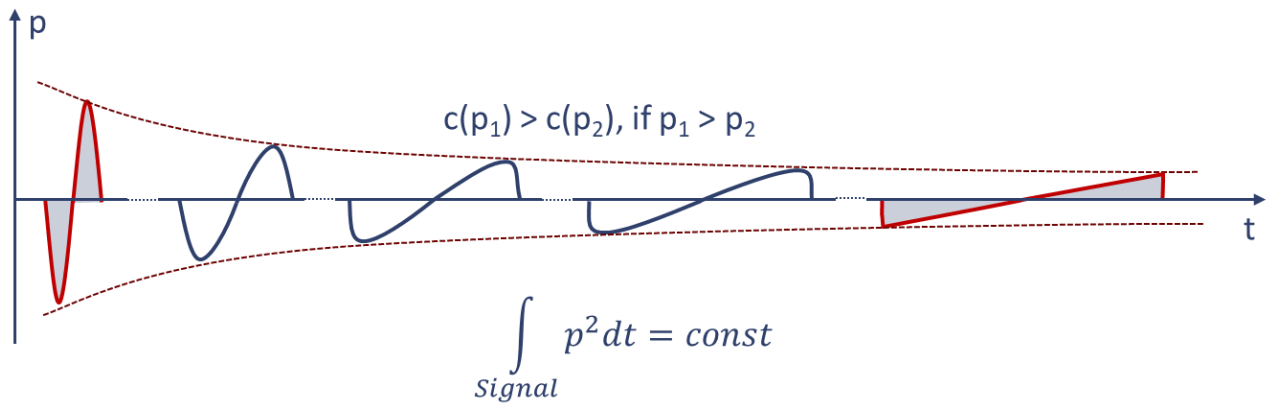


Figure 6 Non-linear change of the shape of a sinus wave to an N-wave

5.2 The N-wave

There are two parameters that define an N-wave of the sound pressure: the peak pressure p_{peak} and the time duration t_c between positive peak and the negative peak, see Figure 7. The progress shown in Figure 6 will continue, of course, even if the signal is a perfect N-wave. During propagation t_c will increase and p_{peak} will decrease.

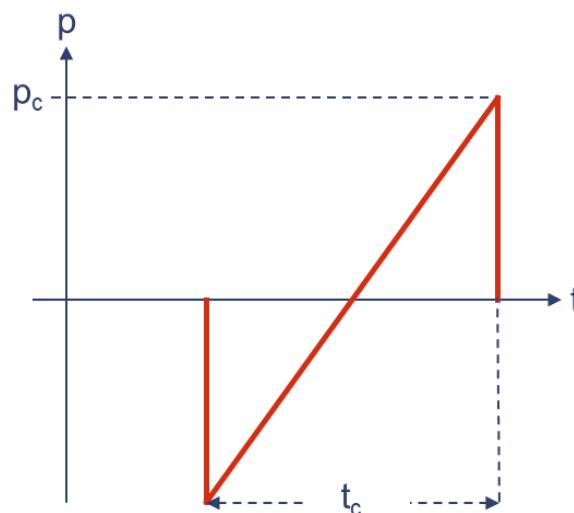


Figure 7 N-wave and its characteristic parameters

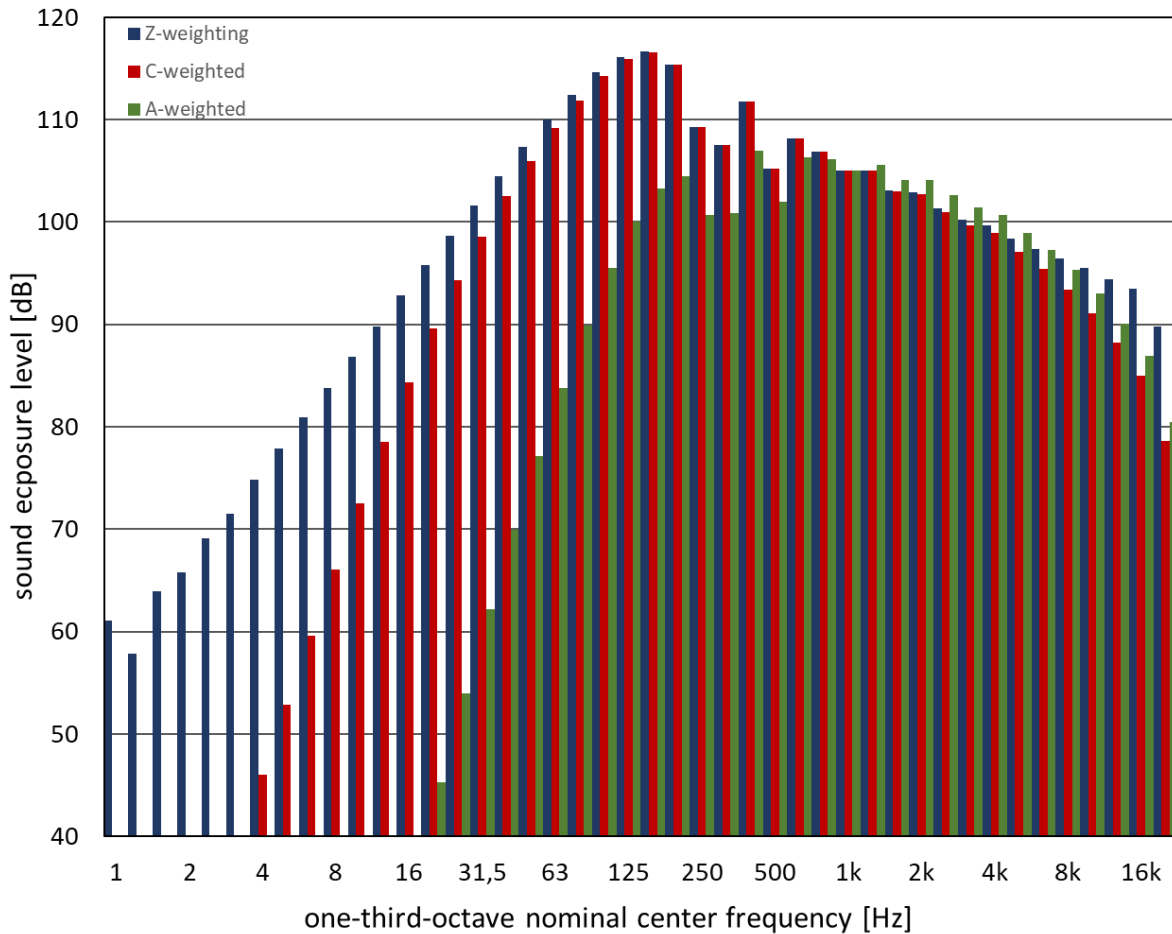


Figure 8 One-third-octave spectrum for a time duration of 1 ms

5.3 The exposition of an N-wave

The pressure exposure E_p of an N-wave is given by Eq. 12.

$$E_p = \int_{N\text{-wave}} p^2(t) dt = \frac{1}{3} p_c^2 t_c \tag{Eq. 12}$$

This formula will help later on to estimate the characteristic pressure if the exposure and the characteristic time duration of the N-wave of projectile sound is known.

5.4 Estimation of the characteristic time duration

The following estimation of time duration of the N-wave is taken from EN ISO 17201 part 4 [4], the pressure model for projectile noise on straight trajectories. In Equation 6 in [4] (here Eq. 15) the time duration is given through the so-called characteristic frequency f_c given in Eq. 13.

$$f_c = \frac{1}{t_c} \quad \text{Eq. 13}$$

$$f_c = f_0 \frac{(M^2 - 1)^{\frac{1}{4}} l_p^{\frac{1}{4}} r_0}{M^{\frac{3}{4}} d_p^{\frac{1}{4}} r^{\frac{1}{4}}} \quad \text{Equation 6 of EN ISO 17201 part 4} \quad \text{Eq. 14}$$

$$t_c = \frac{1}{f_0} \frac{M^{\frac{3}{4}} d_p^{\frac{1}{4}} r^{\frac{1}{4}}}{(M^2 - 1)^{\frac{1}{4}} l_p^{\frac{1}{4}} r_0} \quad \text{Eq. 15}$$

In Eq. 15, let r_0 denote the unit length, r the propagation distance and let denote f_0 the so-called reference frequency. According to chapter A.3 in [4], the reference frequency depends on the speed of sound and on constants that considers the shape of the projectile. In this context f_0 is treated as constant and set to 175,2 Hz assuming streamlined projectiles at 10°C.

The geometry of the projectile is introduced through so-called ‘effective’ parameters, the ‘effective length’ l_p and the ‘effective diameter’ d_p of the projectile. This setting should not be confused with the ‘natural’ geometric length and diameter of the projectile.

The effective diameter is the maximum diameter of the projectile. The effective length of the projectile is the distance between its nose and the first occurrence of effective diameter.

Note

For a sphere, for instance, its radius is the effective length. The effective diameter of this projectile is twice the radius.

From Eq. 15 we can deduce the change of the time duration along the propagation of the N-wave. Rewriting Eq. 15 with a constant Γ to substitute all other parameters than the dependency of characteristic frequency is clear.

$$f_c = \Gamma \frac{r_0}{r^{\frac{1}{4}}} \quad \text{Eq. 16}$$

Using Eq. 13 to introduce the time of duration gives Eq. 17.

$$t_c = \frac{1}{\Gamma r_0} \sqrt[4]{r} \quad \text{Eq. 17}$$

5.5 Estimation of the characteristic pressure

EN ISO 17201 part 4 [4] gives an estimation for the so-called source sound exposure level which is the exposure at a distance of 1 m.

$$L_{Ep,bb,i} = L_0 + 10 \lg \left(\frac{d_p^3}{l_p^4 r_0^4} \right) \text{dB} + 10 \lg \left(\frac{M_i^{\frac{9}{4}}}{(M_i^2 - 1)^{\frac{3}{4}}} \right) \text{dB} \quad \text{Equation 5 of EN ISO 17201 part 4} \quad \text{Eq. 18}$$

The index *bb* indicates that the broadband exposure is meant. The constant exposure level is $L_0 = 161,9 \text{ dB re. } 400 \text{ pPa}^2 \text{ s}$.

$$E_{p0} = 400 \text{ pPa}^2 \text{ s } 10^{L_0/10} \quad \text{Eq. 19}$$

Introducing the exposure instead of its level yields Eq. 20.

$$E_{p,bb,i} = E_{p0} \frac{d_p^3}{l_p^4 r_0^4} \frac{M_i^{\frac{9}{4}}}{(M_i^2 - 1)^{\frac{3}{4}}} \quad \text{Eq. 20}$$

Using Eq. 12 the characteristic pressure depends on the exposure according to

$$p_c = \sqrt{3 \frac{E_p}{t_c}} \quad \text{Eq. 21}$$

Using Eq. 15 and Eq. 20 in Eq. 21 yields Eq. 22.

$$\begin{aligned} p_c(1m) &= \sqrt{3 \frac{E_{p0} \frac{d_p^3}{l_p^4 r_0^4} \frac{M_i^{\frac{9}{4}}}{(M_i^2 - 1)^{\frac{3}{4}}}}{\frac{1}{f_0} \frac{M^{\frac{3}{4}}}{(M^2 - 1)^{\frac{1}{4}}} \frac{d_p}{l_p} r^{\frac{1}{4}}}} \\ &= \sqrt{3 f_0 E_{p0} \frac{d_p^2}{l_p^2 r_0^2} \frac{M_i^{\frac{3}{2}}}{(M_i^2 - 1)^{\frac{1}{2}}}} \\ &= \sqrt{3 f_0 E_{p0} \frac{d_p}{l_p^{\frac{1}{4}} r_0^{\frac{3}{4}}} \frac{M_i^{\frac{3}{4}}}{(M_i^2 - 1)^{\frac{1}{4}}} \end{aligned} \quad \text{Eq. 22}$$

The deduction and reduction are shown in detail to indicate that the always present exponents for length, diameter and MACH-number can be rather confusing. The following chapter about a technical model will use the energy model in EN ISO 17201-2 to determine the exposure and the pressure model to determine the features of the time signal.

WHITHAM gives in [5], [6] a formula for the characteristic pressure of the N-wave of the projectile sound depending on the length of the propagation path for a projectile of length l and diameter d at a speed of M .

$$P_{c,Whitham}(r) = 0,54P_{atm} \frac{d}{l^{\frac{1}{4}}} \frac{M^{\frac{3}{4}}}{(M^2 - 1)^{\frac{1}{4}}} \frac{1}{r^{\frac{3}{4}}} \quad \text{Eq. 23}$$

The comparison of both formulae for the distance of 1 m shows the way

$$0,54P_{atm} = \sqrt{3f_0E_{p0}} \sqrt[4]{\frac{l_{ISO17201}}{l_{Whitham}}} \quad \text{Eq. 24}$$

Eq. 25 inputs the numbers to allow the reader a direct comparison.

$$0,54 \cdot 101300 \text{ Pa} = \sqrt{3 \cdot 175,2 \cdot 400 \text{ pPa}} 10^{16,19} \sqrt[4]{\frac{l_{ISO17201}}{l_{Whitham}}} \quad \text{Eq. 25}$$

$$\frac{54702}{57063} = 0,9586 = \sqrt[4]{\frac{l_{ISO17201}}{l_{Whitham}}}$$

Note

For typical projectile of a gun the effective diameter in EN ISO 17201-4 is equal to the geometric diameter and the effective length in EN ISO 17201-4 is roughly half of the geometric length. Therefore, the 4th root of the length ratio is approximately 0,84 which would lead to 47984 for the right side of the equation.

It is typical for the theories and formulae around the sonic boom or projectile sound that they mostly do not match due to a lot of different assumptions and approximation of the trajectory, geometry and arbitrary environmental conditions.

6 Technical model to predict sound levels

6.1 The need of a technical model

In some countries, the scheme of ISO 9613 or similar models are used to predict long term average receiver levels for noise assessment purposes. In Germany, the application of the scheme of the DIN ISO 9613-2 is mandatory for all industrial noise sources. This includes projectile sound as a component of shooting noise.

The scheme of the ISO 9613 is strictly linear. That means, the source signal cannot change its spectrum due to non-linear effects. Hence, a technical model for the propagation of projectile sound needs a linear regime to correct sound levels for air absorption, barrier effect and so on.

6.2 Concept for a general linear model for projectile sound

Though the scheme of EN ISO 17201 part 4 includes special hint for the application of air absorption and shielding it is not applicable to all trajectories. The scheme in part 2 expects straight trajectories and a constant projectile speed reduction along the trajectory. Hence, part 2 is applicable (and made for) flat shot where the exterior ballistic does not play any role. This is good enough for small arm on short ranges. However, the scheme is not applicable to for range shots, large weapon firing and artillery trajectories.

To archive a technical model that compares to the models to describe other industrial noise source the following concept will use the energy model of part 1 und estimate the linearized spectrum using part 4.

The energy-based estimation of the exposure of the projectile sound at a receiver point does not introduce any propagation features. The non-linear acoustical regime, in particular close to the trajectory does not matter. This is an advantage of energy models over sound pressure models.

An energy model needs a pressure model to deduce the spectrum. The propagation of the pressure is determined through non-linear effects. EN ISO 17201 states that for projectile sound the propagation regime can be assumed to linear if the sound pressure is not higher than 100 Pa. This is the key information we can use to setup a linear model that should be a reasonable approach for all distances in term of a technical model.

We will use the Whitham formula for the characteristic pressure that was already introduced and discussed in a note in chapter 5.5.

Note

This is the easiest way to calculate the distance after which the characteristic pressure is smaller than the limit of non-linearity. However, it would also be possible to use the pressure prediction of part 4 of the EN ISO 17201 series.

6.3 On how to estimate a limit of linearity

We will start again with WHITHAMS formula for the peak pressure P_c of the projectile sound Eq. 23 and solve the formula for the distance r .

$$r = \left(0,54 \frac{P_{atm}}{p_{c,Whitham}} \right)^{\frac{4}{3}} \sqrt[3]{\frac{d_{Whitham}^4}{l_{Whitham}} \frac{M^3}{(M^2 - 1)}} \quad \text{Eq. 26}$$

Setting $p_{c,Whitham}$ to $p_{lin} = 100 \text{ Pa}$, the so-called limit of non-linearity for projectile sound according to EN ISO 17201 series yield an estimation r_{lin} . For distances greater than r_{lin} the propagation is said to be linear.

$$r_{lin} = \left(0,54 \frac{P_{atm}}{p_{lin}} \right)^{\frac{4}{3}} \sqrt[3]{\frac{d_{Whitham}^4}{l_{Whitham}} \frac{M^3}{(M^2 - 1)}} \quad \text{Eq. 27}$$

For a technical model with propagation-independent signal shape it is reasonable to fix the shape just at the edge of linearity. Eq. 15 estimates the characteristic time duration of the N-wave t_c dependent on the distance. Fixing the distance to just that edge of linearity we apply Eq. 27 to Eq. 15. In Eq. 15 will change the symbols for projectile diameter and length to be clear. For the following, let denote $l_{ISO17201} \equiv l_p$ and let denote $d_{ISO17201} \equiv d_p$

$$t_{clin} = \frac{0,0467 \text{ s}}{r_0} \frac{M}{(M^2 - 1)^{\frac{1}{3}}} \frac{d_{ISO17201}^{\frac{1}{3}} d_{Whitham}^{\frac{1}{3}}}{l_{ISO17201}^{\frac{1}{4}} l_{Whitham}^{\frac{1}{12}}} \quad \text{Eq. 28}$$

Eq. 28 comes up with two measures for the diameter and length of the projectile. In the discussion that led to Eq. 25 we got an idea what the difference is. Let us assume for a moment that $l_{ISO17201} = l_{Whitham} = l$ and that $d_{ISO17201} = d_{Whitham} = d$ the result is Eq. 29

$$t_{clin} \approx 0,0467 \text{ s} \frac{M}{r_0} \sqrt[3]{\frac{d^4}{l(M^2 - 1)}} \quad \text{Eq. 29}$$

In EN ISO 17201 part the formula for t_{clin} (reprinted here as Eq. 30) looks a little bit different.

$$t_{clin,ISO17201} \approx 15 \frac{M}{c_0} \sqrt[3]{\frac{d^4}{l(M^2-1)}} \quad \text{from EN ISO 17201 part 2} \quad \text{Eq. 30}$$

If we set

$$t_{clin,ISO17201} \approx 0,0441 \frac{M}{r_0} \sqrt[3]{\frac{d^4}{l(M^2-1)}} \quad \text{from EN ISO 17201 part 2, } c_0 = 340 \frac{\text{m}}{\text{s}} \quad \text{Eq. 31}$$

The differences in these result are not significant in terms of a linear model for projectile noise. Hence, Eq. 32 and Eq. 33 are sufficient approximation for a technical model to fix the shape and the spectrum of N-wave.

$$t_{clin} = 0,045 \frac{M}{r_0} \sqrt[3]{\frac{d^4}{l(M^2-1)}} \quad \text{Eq. 32}$$

$$f_{clin} = 22 \frac{r_0}{M} \sqrt[3]{\frac{l(M^2-1)}{d^4}} \quad \text{Eq. 33}$$

7 Discussion

7.1 The relevant parameters of a projectile

This chapter should normally precede all the chapters that introduce projectile sound models. These models use parameters to describe the velocity, the drag along the trajectory and, of course, the geometry of the projectile. It is put at the end because the definition of these parameters is the root of ambiguities in the formulae. Therefore, it was more helpful to let the reader assume that all these parameters are clear. However, there are not, at least to the author.

7.2 The MACH number

It seems to reasonable to describe the speed of the projectiles in terms of its ratio to the speed of sound. All phenomena around the sonic boom and the projectile sound depends on this ratio and not on the speed directly. Hence, in all formulae the MACH number depicts the speed of the projectile. However, using this measure conceals a major problem.

We can easily measure the projectile speed, for sure. However, what about the ‘speed of sound’. This speed is normally said to be a constant for a given ambient temperature and ambient pressure. When the projectile penetrates the air body it will compress the air at its tip. As a consequence, locally to the tip the air will heat up because air is not an ideal gas. At higher pressure and in particular at higher temperatures the speed of sound will rise. And the MACH number will not be what we expect. At the tail of the projectile there is a drop of pressure and a drop of temperature causing the MACH number to increase. Within the air flow along the projectile – before and after it passes the maximum diameter of the projectile at the effective length – the author is not really sure.

It is rather interesting to just look at bodies moving through with speeds close to the speed of sound of the undisturbed air. MCCOY gives in his book on ‘Modern Exterior Ballistics’ [7] a lot of shadowgraphs of the flow field of bodies at different speed. These graphs show pressure changes and therefore indicate the radiation of sonic boom from the body as more or less contoured stripes.

Note

Anyway, MCCOYS text book is recommended to get into the calculation of trajectories and forces that act on a projectile during its flight.

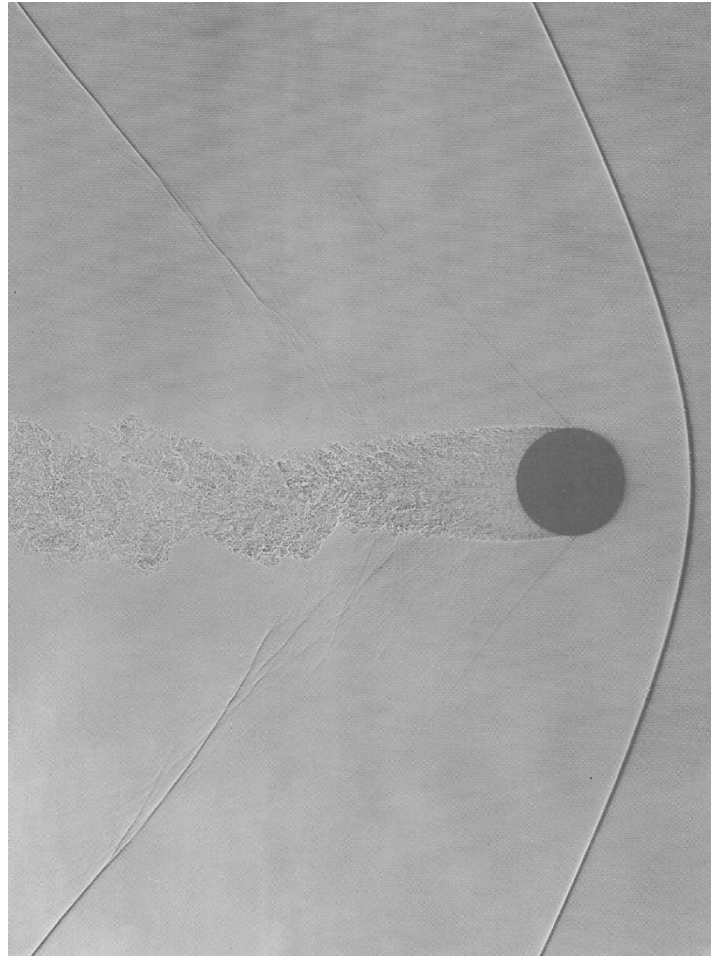


Figure 9 Shadowgraph of 7/8 inch smooth sphere at Mach 1,24, after MCCOY [7]

Figure 9 shows the shadowgraph of a sphere at 1,24 MACH moving from left to right. First of all, there is a clear positive shock front ahead of the sphere. The turbulence behind the sphere obviously generates a second clear shock. This shock front moves at a lower speed than the first one. The time difference between the two increases with increasing distance from the trajectory. There is a third observation. Just when the sphere reaches its maximum diameter there is weak front that is traveling at a speed that compares to the speed of the front out of the turbulence.

After some distance one can assume that there is an N-wave with in increasing time duration between the first shock wave and the shock wave from the turbulence. The N-wave duration can obviously not be directly estimated on the diameter or length of the sphere.

For a cylinder-shaped projectile at 1,04 MACH, Figure 10 shows a very interesting behavior. The first shock front is nearly one cylinder-length ahead. The second front stems somewhere from the surface of the body. There is no change in diameter but there is presumably a change in the local sound speed.

The reader might check the following hypothesis: Sphere and cylinder compress the air in front of them which will heat up and compress the air and, of course, will increase the sound speed in that region. Therefore, for this region the body is not supersonic but subsonic and the sound can travel faster than the body. The shock generates just when the waves from the body enter a region where they come together due to the lower temperature and lower pressure domain in front of the projectile.

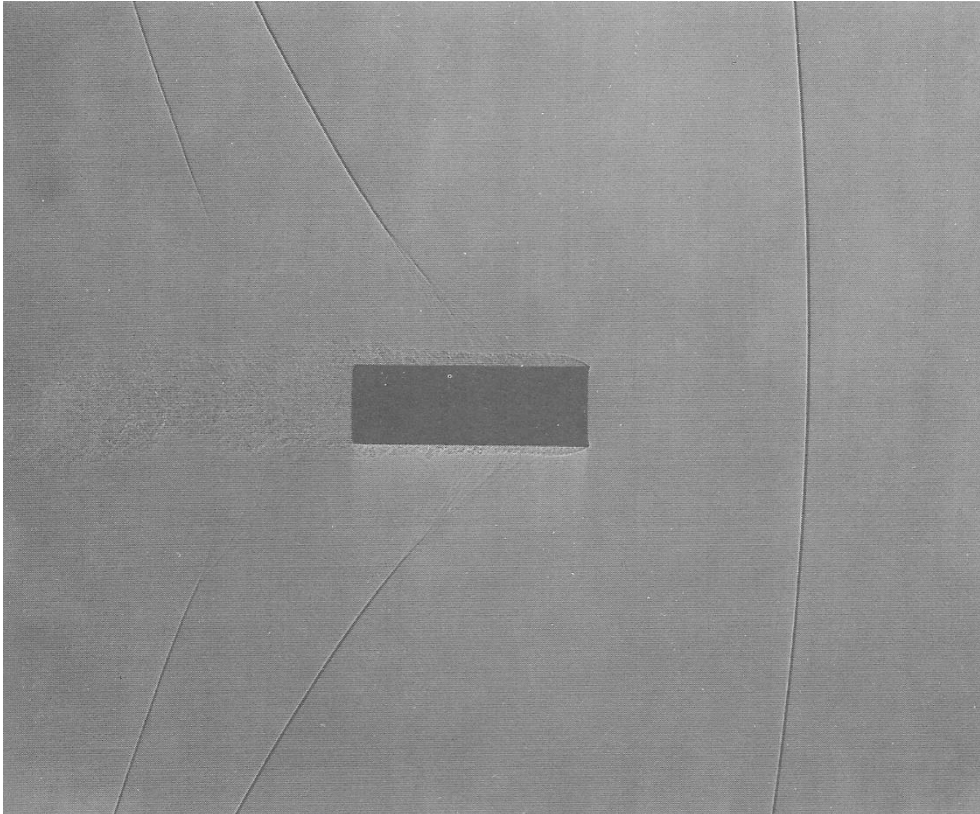


Figure 10 Shadowgraph of a cylinder at Mach 1,04, after MCCOY [7]

Looking at the cylindrical surface, the body has a skin of turbulent air that continues to widen until the tail turbulence takes over. It seems that the second shock wave generates at half the way from nose to tail, which may be called the 'effective length' though there is no change in diameter at all.

The following series of shadowgraphs shows a projectile at increasing speeds, Figure 11. Even at 0,89 MACH there is a strange shock wave at that position of the projectile where the diameter decreases clearly. This is the first brick in the sound, so to say. The sound from the tip and from the surface cannot propagate to the tail and act like a 'normal' sound source. Due to the low pressure and low temperature region behind the projectile the sound speed is too slow and the sound waves pile up there.

Increasing the speed up to 1 MACH the graphs show more and more bricks of the wall. Obviously, these shock fronts accompany the projectile; they are not propagating into the vicinity. They behave like local standing waves. This phenomenon is the reason for the steep increase of the drag coefficient of the body at speeds just below the speed of sound.

The graph for 1,02 MACH is the first figure that indicates a shock front ahead the projectile. At higher speeds this shock front comes closer and closer to the tip of the projectile. The origin of the negative part of the N-wave really develops at the effective length of the projectile (which is the length from nose to that position along the projectile where the diameter gets smaller again), at least at 1,06 MACH. At 2,66 Mach the origin is more the tail turbulence.

7.3 Resumé

The MACH number of the projectile as the ratio of the speed of the projectile to the speed of sound at ambient air conditions is an important and significant measure to scale projectile sound. However, the understanding the fine structure in the direct vicinity of the projectile needs to discuss the speed of sound and its dependency on pressure and temperature.

This chapter makes clear, that any modelling projectile sound is really complex. The shape of the body plays an important role. The non-linear sound propagation helps to get rid of any fine structure close the projectile. Hence, we end up with an N-wave with two simple parameters, the peak pressure and the time duration.

It is also clear, that the prediction of these two parameters is a challenge. The formulae introduced above are approximations. Models can use the effective length or the true length. There may be situation where one approach is better than the other and vice versa.

The prediction of the energy has some advantages over the prediction of pressures. The energy integrates over a lot of local problems. However, it must be clear that the drag coefficient is the key parameter that again depends on shape and speed.

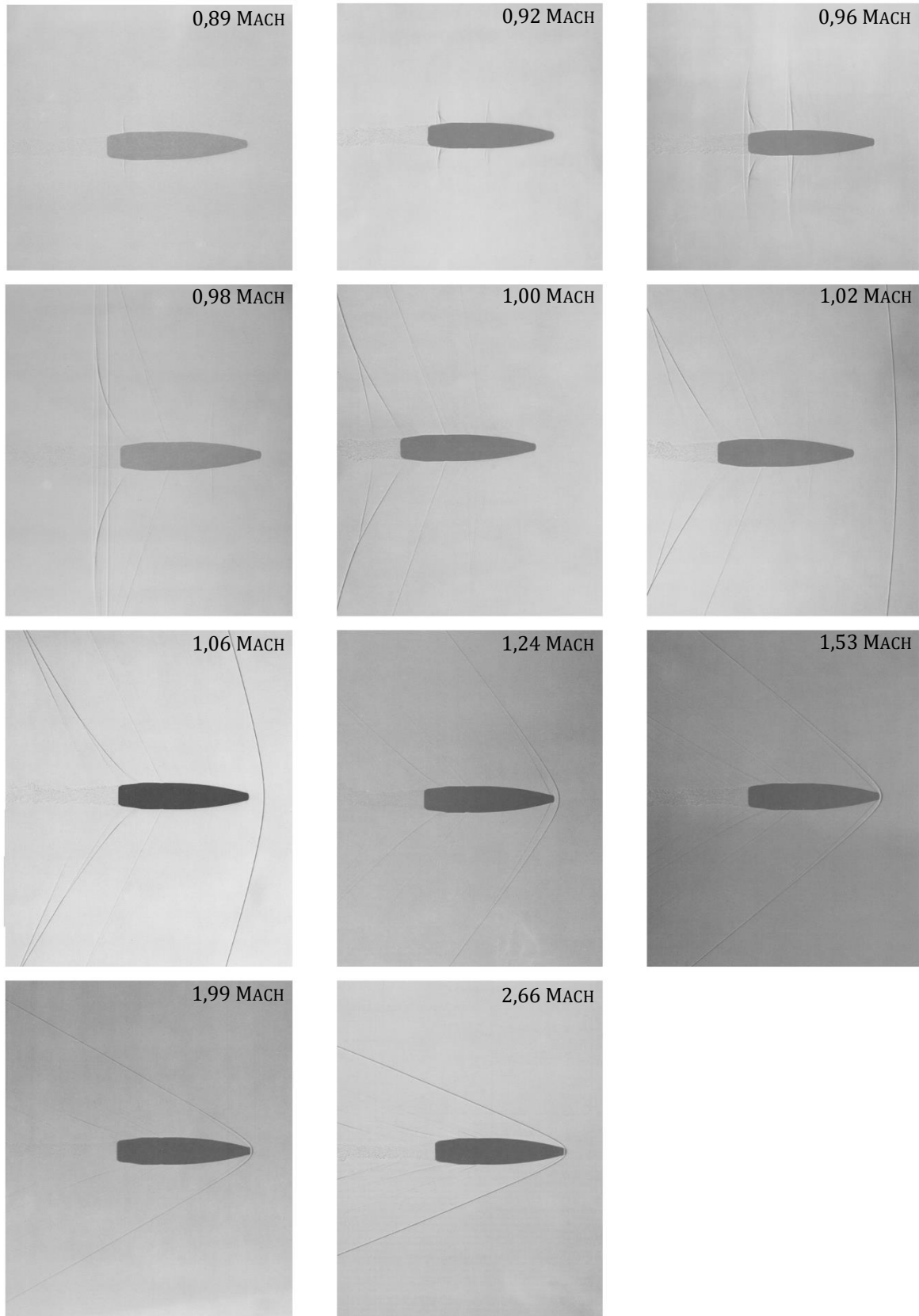


Figure 11 Shadowgraph of the same projectile at different speed, compiled graphs after MCCOY [7]

8 Example

8.1 Howitzer

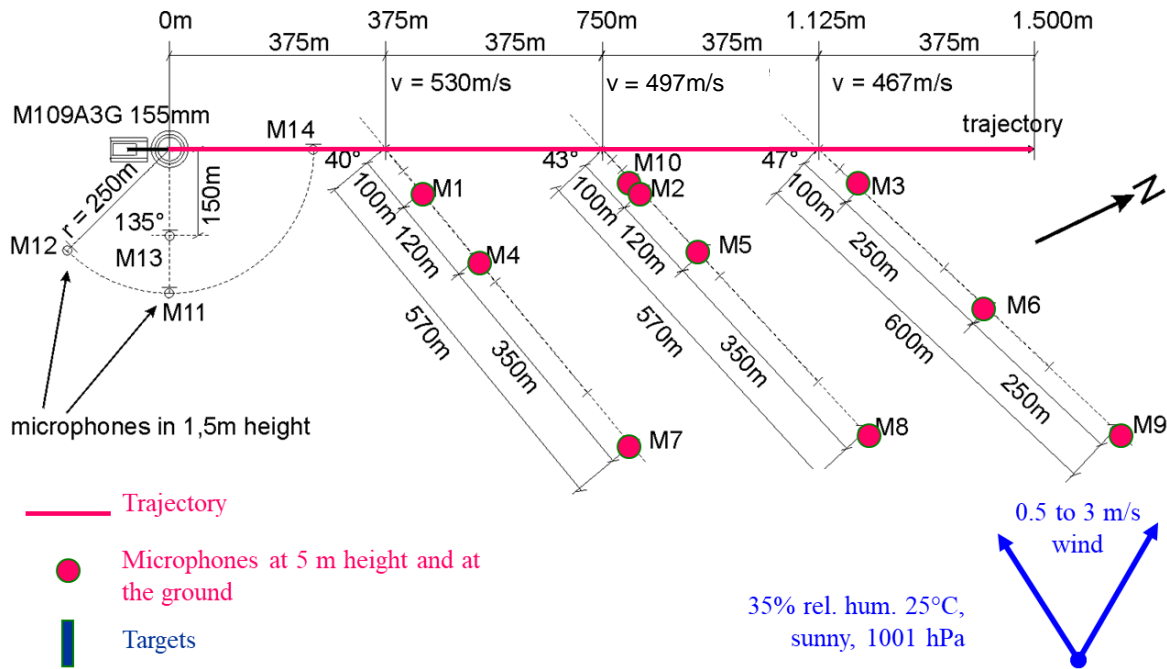


Figure 12 Test plan of a projectile sound measurement of flat howitzer shots, after BUCHTA and HIRSCH [8]

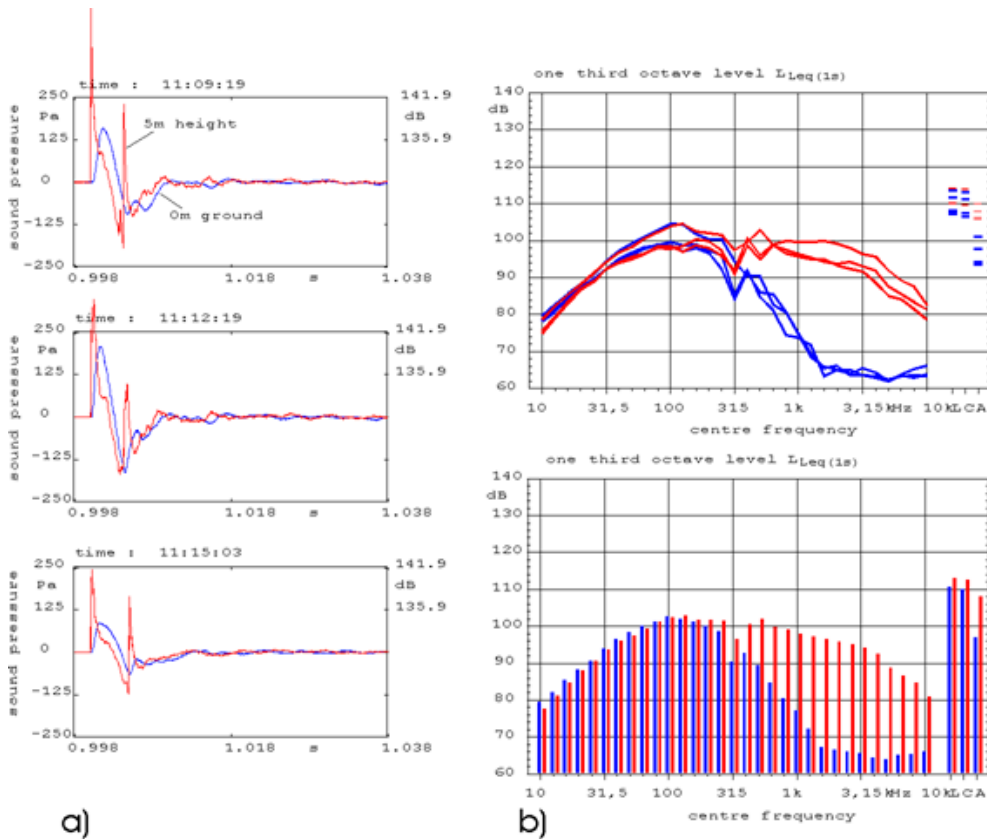


Figure 13 Projectile sound of flat howitzer shot at M2, after BUCHTA and HIRSCH [8]
 a) unweighted pressure time histories at the ground (0 m) and at 5 m height
 b) one third octave spectra (top graph) and average spectrum (bottom graph)

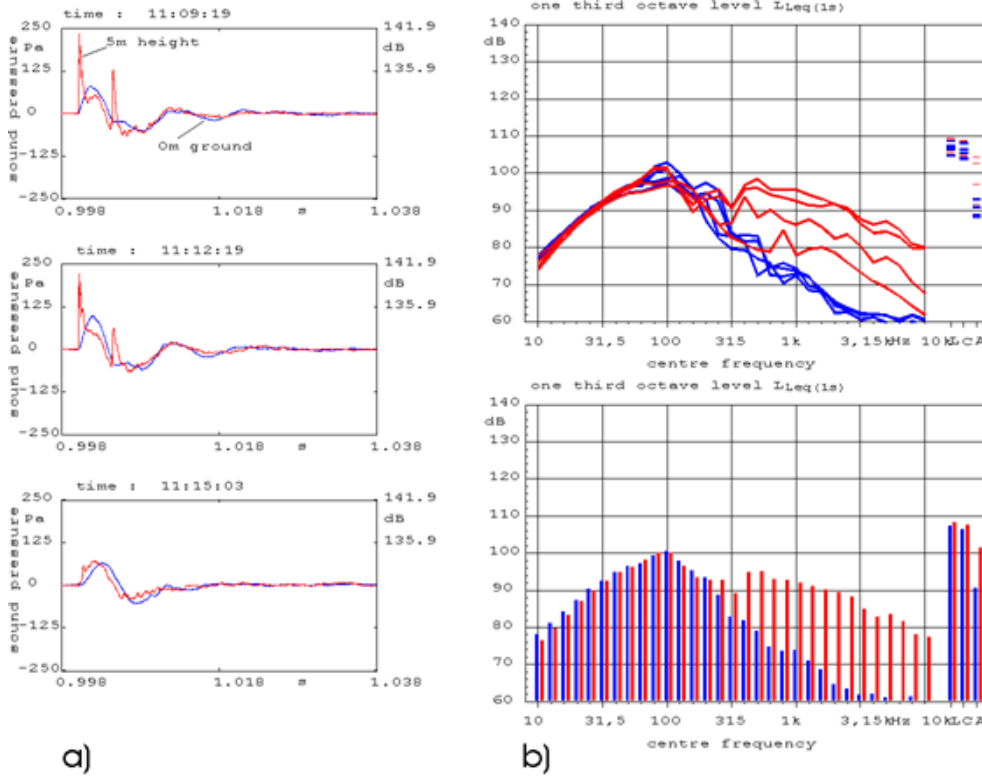


Figure 14 Projectile sound of flat howitzer shot at M5, after BUCHTA and HIRSCH [8]
 a) unweighted pressure time histories at the ground (0 m) and at 5 m height
 b) one third octave spectra (top graph) and average spectrum (bottom graph)

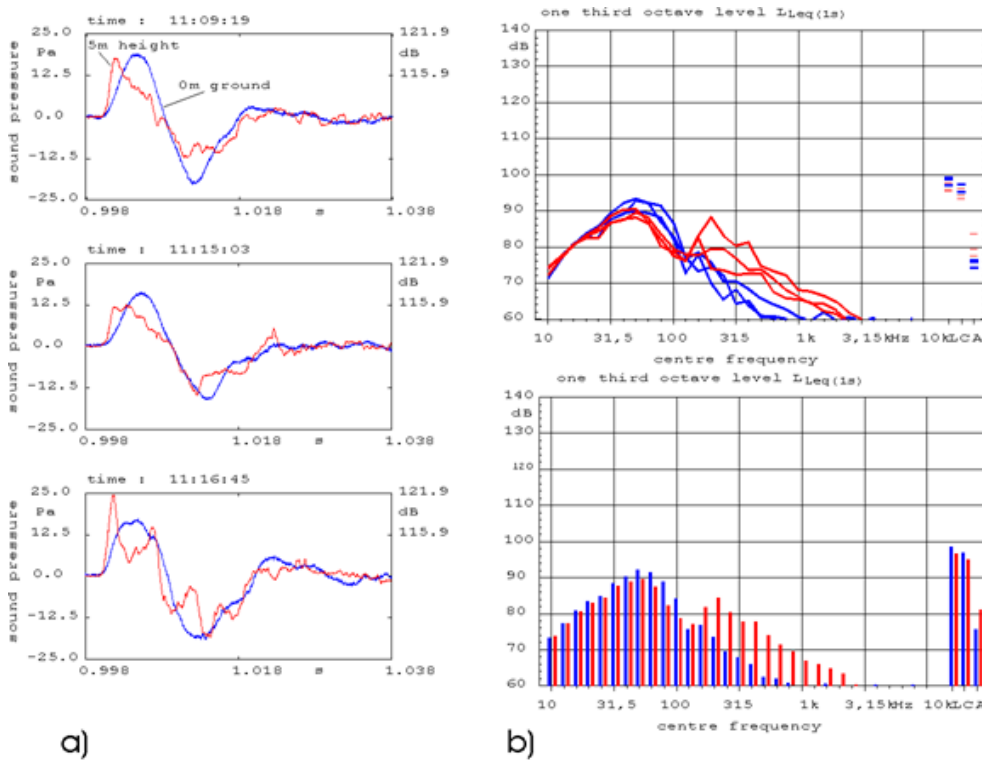


Figure 15 Projectile sound of flat howitzer shot at M8, after BUCHTA and HIRSCH [8]
 a) unweighted pressure time histories at the ground (0 m) and at 5 m height
 b) one third octave spectra (top graph) and average spectrum (bottom graph)

Most investigations on projectile sound are done by the military. Sharing theory and models normally is not restricted but real measurements are in most cases confidential. For sure, there are reports that consider projectile sound analysis of civil weapons. However, in such reports a lot of information about the trajectory, the projectile features including for instance the drag coefficient function is missing. Therefore, the following example is based on a published investigation on flat howitzer shots, BUCHTA and HIRSCH [8]. Nevertheless, the author wants to confirm that the given example and the uncertainties of the prediction is representative also for application to small handheld civil weapons.

Note

Chapter 8.2 presents some high-resolution pressure time histories of calibre 5.56 rifle shot.

This chapters reports on a measurement of the projectile sound of flat howitzer shots on targets at 1200 m distance. The shell will not explode at the targets but penetrate them and will continue flying before the explode at the ground. The test plan is depicted in Figure 12 providing most of the information including the projectile speed at the relevant source position and the expected direction of projectile sound propagation. The mass of the projectile is ≈ 42 kg

The following figures show the measurement results for three shots in term of sound pressure history and one-third octave. Both, sound pressure and spectra are given unweighted. Note that the color red always indicates the results at 5 m height and the color blue indicates the results measured at the ground.

The time histories either at 5 m height nor at the ground are looking like N-waves. In particular at the ground, one would expect simple pressure doubling and therefore a signal that is not disturbed by the ground reflection. Both statements do not hold. The following discussion will point out the way how these measurements have to be analysed to yield reliable results for p_c and t_c .

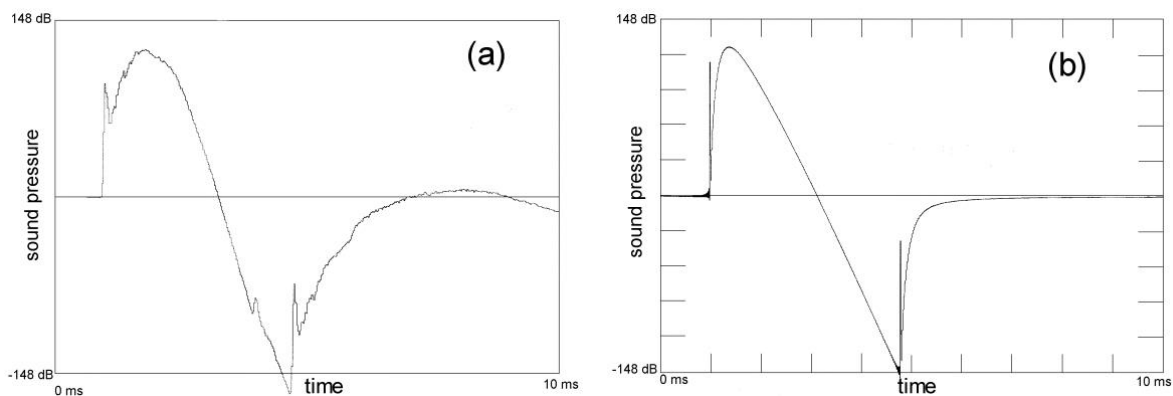


Figure 16 Projectile sound of flat howitzer shot at M10, after HIRSCH and BUCHTA [9]
 a) measured unweighted pressure time history at the ground
 b) calculated unweighted pressure time histories

Figure 16 exemplary shows the pressure signal at $r = 88$ m distance. The source point of the projectile sound is indicated in Figure 12. The trajectory is 8 m high with a speed of $M = 1.46$. The microphone lays directly on the grassy ground. Obviously, this is not an N-wave. The characteristic measures p_c and t_c cannot be directly read from this signal because the ground effect will cancel out most of the higher frequencies due to the flat angle of incidence.

Choosing an N-wave of $p_c = 330$ Pa and $t_c = 3,955$ ms and applying the theory the reflection of spherical waves at a complex impedance ground using some standard parameters for grass yield the superimposed signal in graph b of Figure 16. Measurement and calculation agree sufficiently to state that the chosen N-wave of the given parameters is a good estimation.

	1	2	3	4
1	Symbol	Reference	Unit	Value
2	v	projectile speed	m/s	497
3	m	projectile mass	kg	43,1
4	d	projectile diameter	m	0,155
6	l	projectile length l_{WIRTHAM}	m	0,5
7	l_{eff}	projectile length l_{ISO17201}	m	0,25
8	A	projectile area	m ²	46,8
9	θ_e	Eq. 2 at segment end	°	46,7896
10	θ_b	Eq. 2 at segment begin	°	46,7988
11	$s_0 \equiv r_0$	Length unit, length of segment	m	1
12	M_b	MACH number at segment begin	1	1,46079
13	M_e	MACH number at segment end	1	1,46054
14	C_w	drag coefficient along segment	1	0,357
15	t_{clin}	Eq. 31	ms	6,5
16	f_{clin}	Eq. 32	Hz	152
17	r_{lin}	Eq. 27	m	657,5
18	Q	Eq. 4	J	1990,6
19	Q	Eq. 5	J	1990,6
20	ΔE_{kin}	Loss of kinetic energy	J	1773,0
21	σ_{ac}	acoustical efficiency	%	10
22	$\kappa_{\text{ISO17201-4}}$	Change of speed per one meter	1/s	-0,085
23	$L_{\text{Ep,bb,i}}$	Eq. 12 Part 4 exposure level	dB	145,4

Table 1 Some model results for howitzer signals

	1	1	3	4	5	6
1	Measure	Unit	M10	M2	M5	M8
2	r	m	88	100	220	570
3	$S_{cylinder}$	m ²	295,0	335,0	735,7	1904,2
4	S_{Wedge}	m ²	5,7	7,4	35,6	239,2
6	E	Pa ² s	270,1	237,2	105,3	37,9
7	L_E	dB	118,3	117,7	114,2	109,8
8	P_{peak}	Pa	405,3	373,7	225,6	120,2
9	$P_{c,Whitham}$	Pa	451,9	410,6	227,3	111,3
10	$A_{nlin,ISO17201-4}$	dB	4,85	4,99	5,84	6,85
11	$L_{E,ISO17201-4}$	dB	121,0	120,3	116,0	110,5
12	$P_{peak,ISO17201-4}$	Pa	555,7	504,3	275,9	130,8
13	$L_{p,peak,ISO17201-4}$	dB	148,9	148,0	142,8	136,3
14	$f_{c,ISO17201-4}$	Hz	202,7	196,3	161,2	127,0
15	$t_{c,ISO17201-4}$	ms	4,93	5,09	6,20	7,87
16	$t_{c,measured}$	ms	3,95	8	10	20
17	$f_{c,measured}$	Hz (one-third octave)	125	125	100	50
18	$P_{c,measured}$	Pa	330	200	125	25

Table 2 Comparison of model predictions to measured values

It is important to note that the measured signals are typical for the projectile sound. The ground is always present and for flat trajectories the angles of incident is always near grazing incidence. Therefore, the higher frequencies are concealed by the ground reflection. This analysis describe above is necessary in most cases.

Table 2 gives some model results for the howitzer shots measured at the position that receive projectile sound from the same point at the trajectory at 750 m, Figure 12. It is up to reader to do her or his analysis.

Note:

The numbers in Table 2 may give the reader the opportunity to check own calculations for quality assurance purposes. The author calculated the numbers using an Excel sheet. Due to the complex numerics, the results here are not granted.

One interesting result is the comparison of the predicted exposure levels according to ISO EN 17201-2 (including the correction according [1] and [2]) and ISO EN 17201-4, row 25 and row 32 of Table 2. The levels of the energy model in ISO EN 17201-2 are slightly higher. This difference could be easily decreased by decreasing σ_{ac} the fraction of Q that is assumed to convert to acoustical energy. Considering the measurement result, both values slightly too high, round about 3 dB. For noise assessment purposes, expert like to predict a little bit higher levels to be sure that they do not underestimate the noise load.

Though it is clear, that the loss of kinetic energy is a wrong approach for the source energy of projectile sound, it is sometimes the best you can do, due to missing information. The estimation of the kinetic energy loss only needs the mass of the projectile and its speeds at the begin and at the end of the segment under consideration. There is no need for knowledge of the projectiles shape, length or diameter. For the estimation of the geometrical spreading these properties are also sufficient. Therefore, this is the shortest way to get a rough estimate.

Therefore, Table 2 indicates the ΔE_{kin} in row 20 (assuming the mass of the projectile to be 42 kg.) The value directly compares to the values of Q in row 19 or 18. ΔE_{kin} obviously underestimates the exposure by about 10%. For rather straight trajectories and unpropelled projectiles ΔE_{kin} is always a good start.

Note

The calculation of ΔE_{kin} was introduced in ISO EN 17201-2. Most application of the scheme of this standard will rely on this value.

8.2 Close up pressure time histories of the projectile sound of a 5.56 shot

A measuring campaign conducted at the WTD 91, Meppen, primarily focused on the measurement of the detailed directionality of the muzzle blast. Some aspects of this campaign were published in [10].

Figure 17 shows a sketch of the test plan. The pressure histories were recorded along at two measuring circles having 10 m and 20 m radius and for two measuring heights 1 m and 2 m. The .223 rifle (caliber 5.56) fired at the center of the circle at 2 m height over grassy ground.

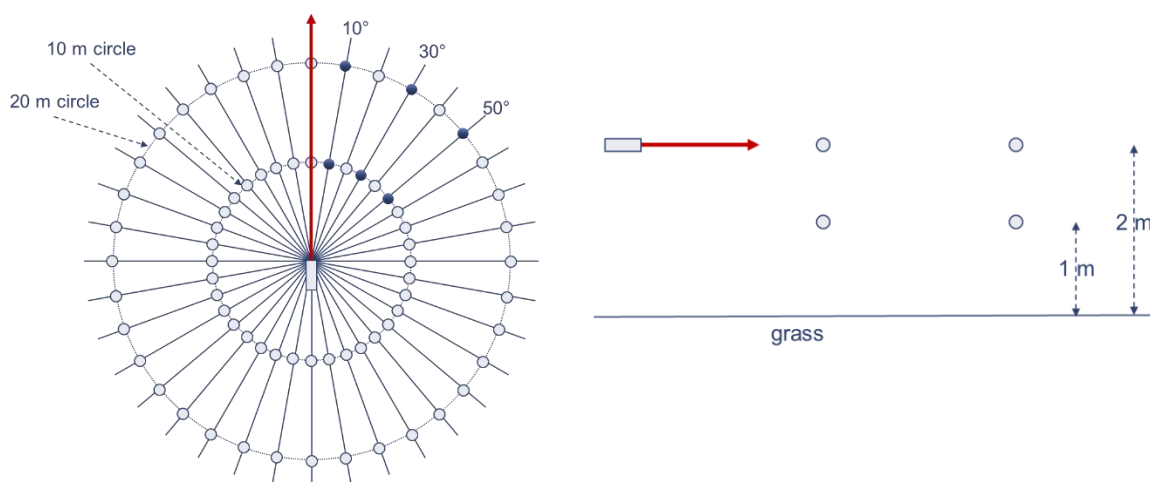


Figure 17 Sketch of the test plan for the detailed measurement of the directionality of a muzzle blast according EN ISO 17201-1

The recorded time histories of the sound pressure also provide the projectile sound at those direction where it occurs. Due to the primary task, the sampling rate of the time history records was chosen to be 100.000 Hz, sufficient for the muzzle blast, a little bit too low for the projectile sound. However, because the shape of the signal is well-known, the low sampling rate does not play a significant role in the following analysis.

The analysis here selects only a representative subset out of the collection of available time histories: at 10°, 1 m and 2 m height at the 10-m and 20-m circle. The following figures combine the time history and the related one-third octave spectrum at each receiver point under investigation. Due to the geometry, there is in most cases a clear separation between the direct sound and the ground reflection. Therefore, time gating was applied to obtain the time history and the spectrum. However, for some reasons the time window for the evaluation of the spectrum is not the same as for the time history. Hence, the results of the lower one-third octaves shown in the figures are strongly influenced by the length of the time gate.

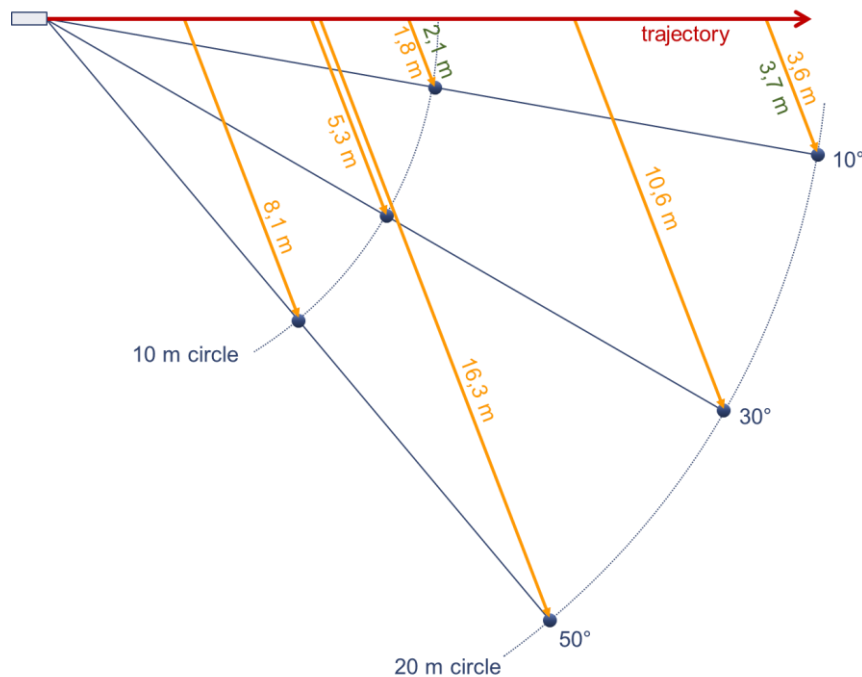


Figure 18 Geometry for the source point and propagation distance of the projectile sound acc. Figure 17, distance formatted in green holds for 1 m receiver point height if it differs significantly from distance to the 2 m measuring height

Figure 18 indicates the propagation situation for the receiver points under consideration. Only for the receivers at 10° the length of the propagation path really differs between the two measuring heights. Hence, only for those receiver points the difference is considered.

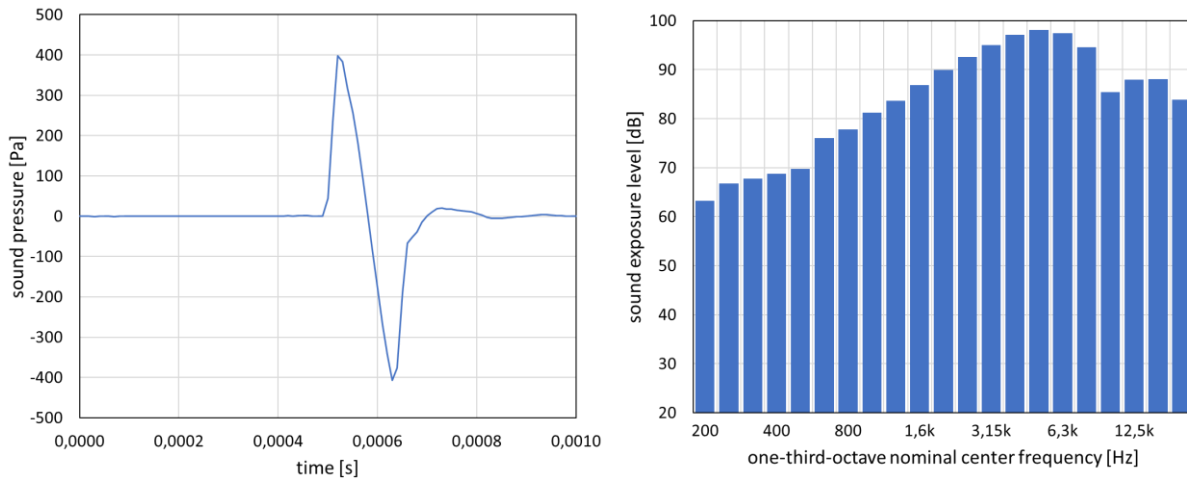


Figure 19 High resolution time history and relevant one-third-octave spectrum measuring circle 10 m at 10°, measuring height 1 m

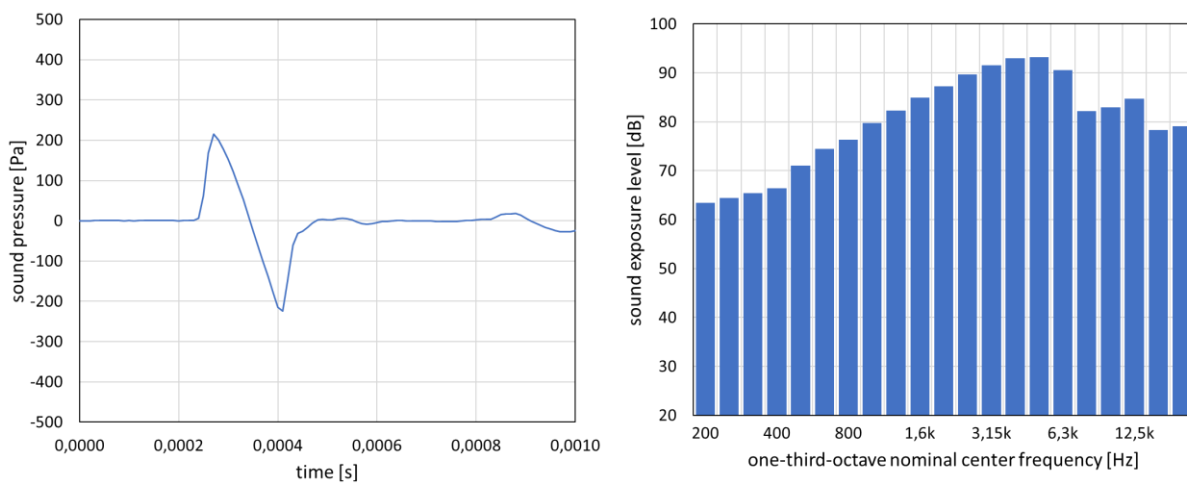


Figure 20 High resolution time history and relevant one-third-octave spectrum measuring circle 10 m at 30°, measuring height 1 m

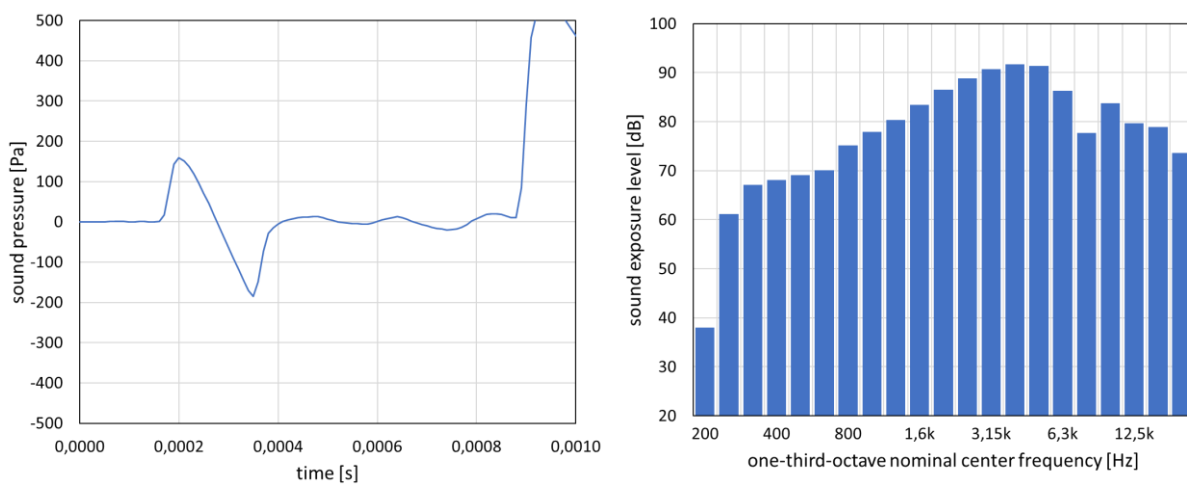


Figure 21 High resolution time history and relevant one-third-octave spectrum measuring circle 10 m at 50°, measuring height 1 m

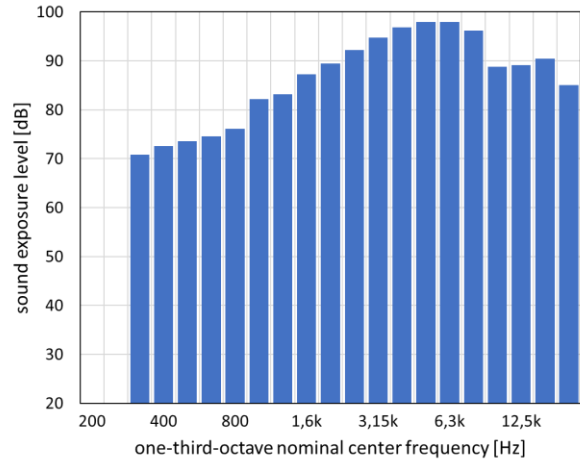
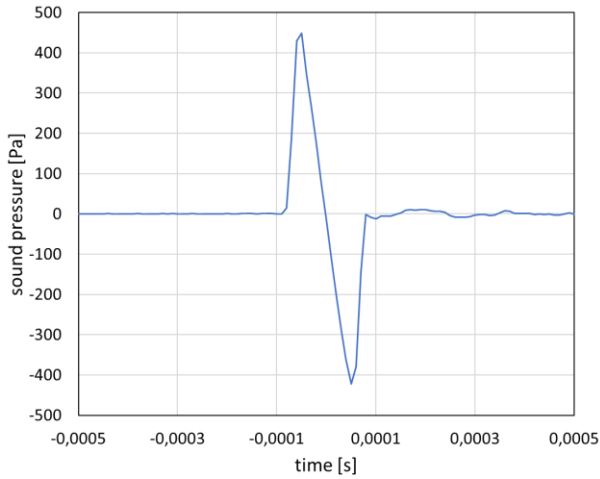


Figure 22 High resolution time history and relevant one-third-octave spectrum measuring circle 10 m at 10°, measuring height 2 m

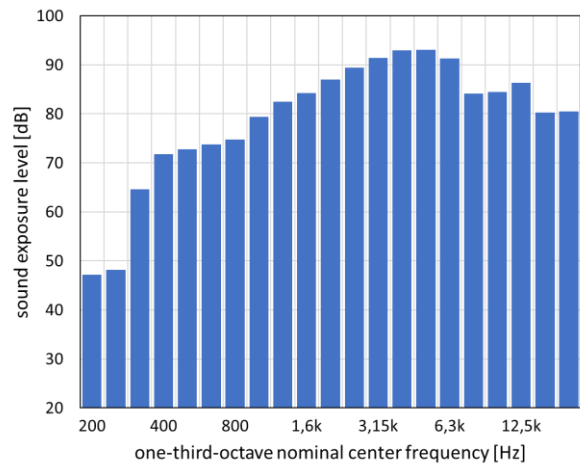
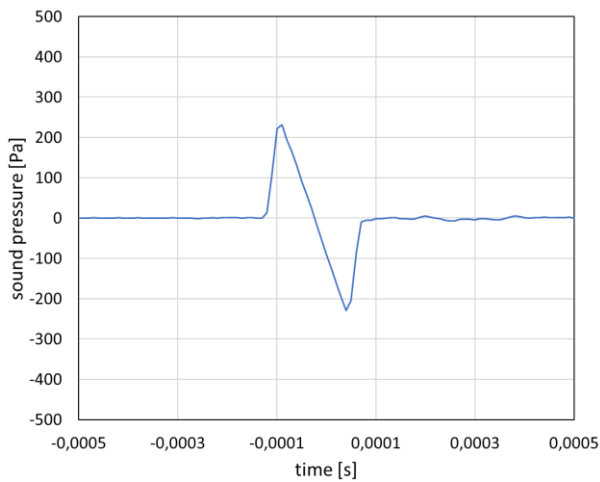


Figure 23 High resolution time history and relevant one-third-octave spectrum measuring circle 10 m at 30°, measuring height 2 m

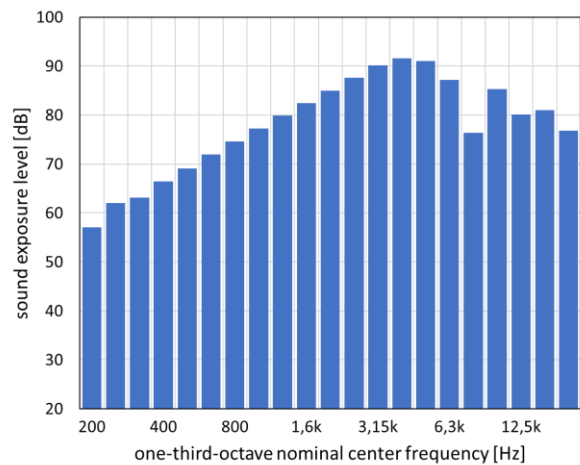
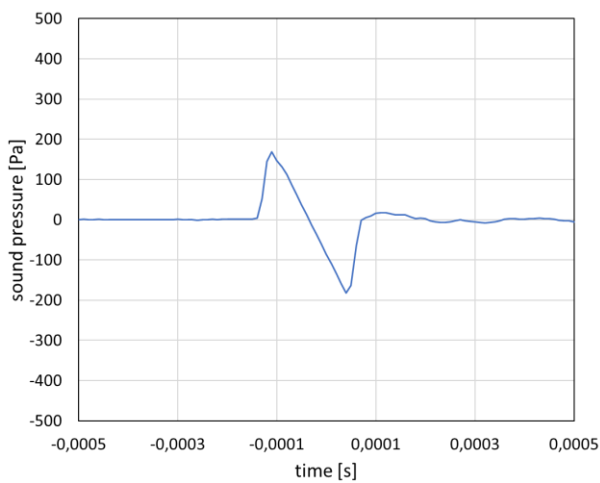


Figure 24 High resolution time history and relevant one-third-octave spectrum measuring circle 10 m at 50°, measuring height 2 m

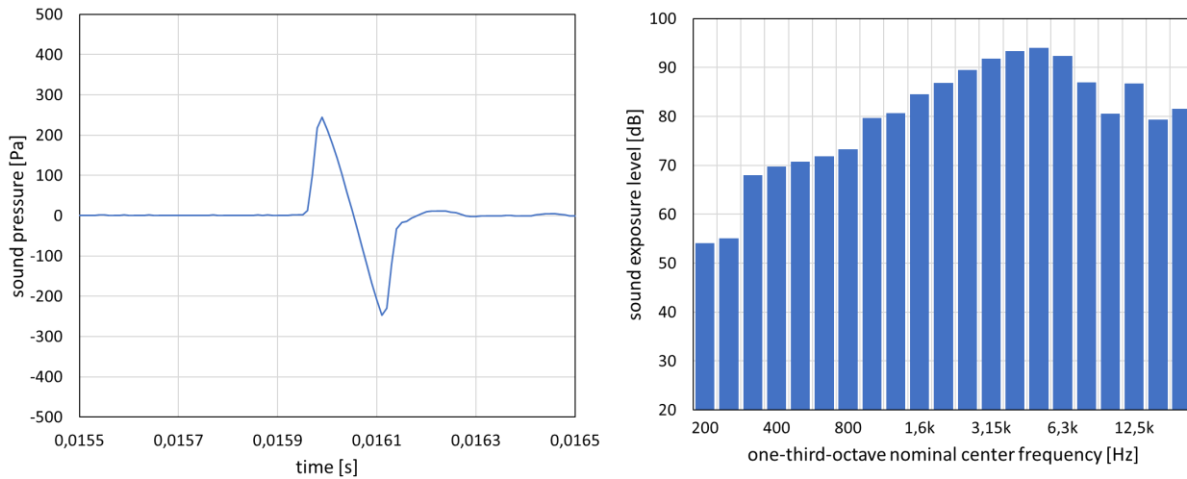


Figure 25 High resolution time history and relevant one-third-octave spectrum measuring circle 20 m at 10°, measuring height 1 m

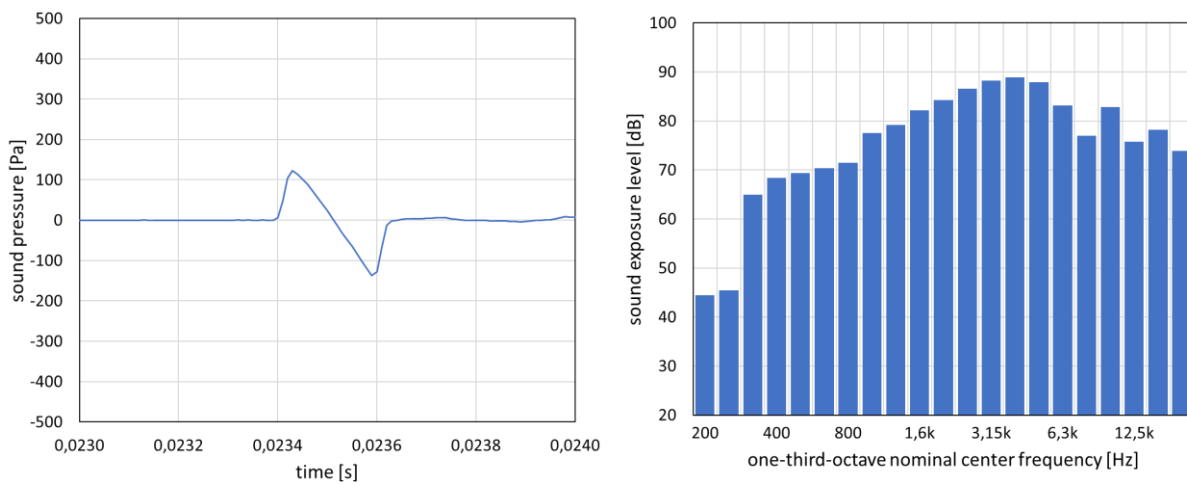


Figure 26 High resolution time history and relevant one-third-octave spectrum measuring circle 20 m at 30°, measuring height 1 m

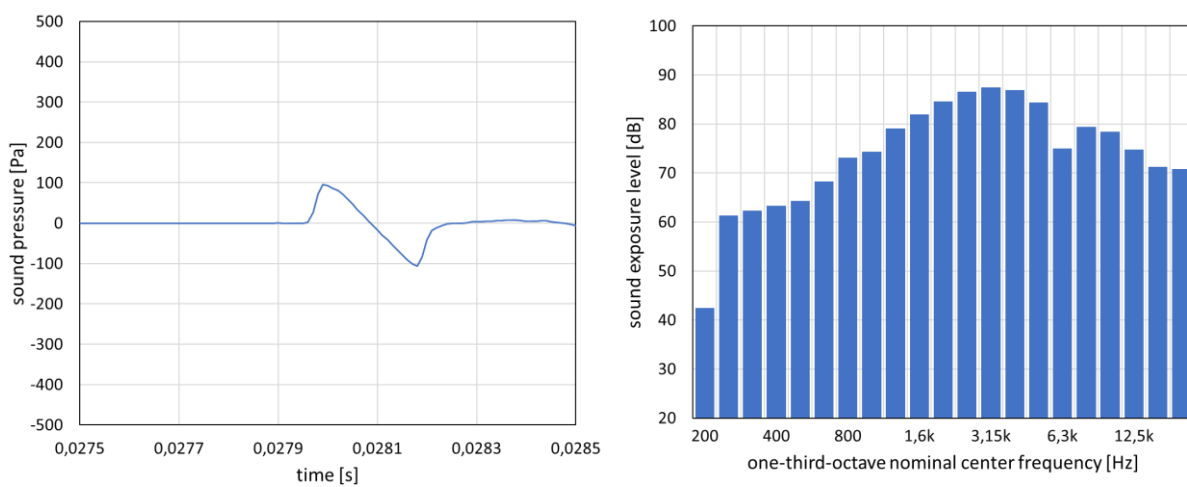


Figure 27 High resolution time history and relevant one-third-octave spectrum measuring circle 20 m at 50°, measuring height 1 m

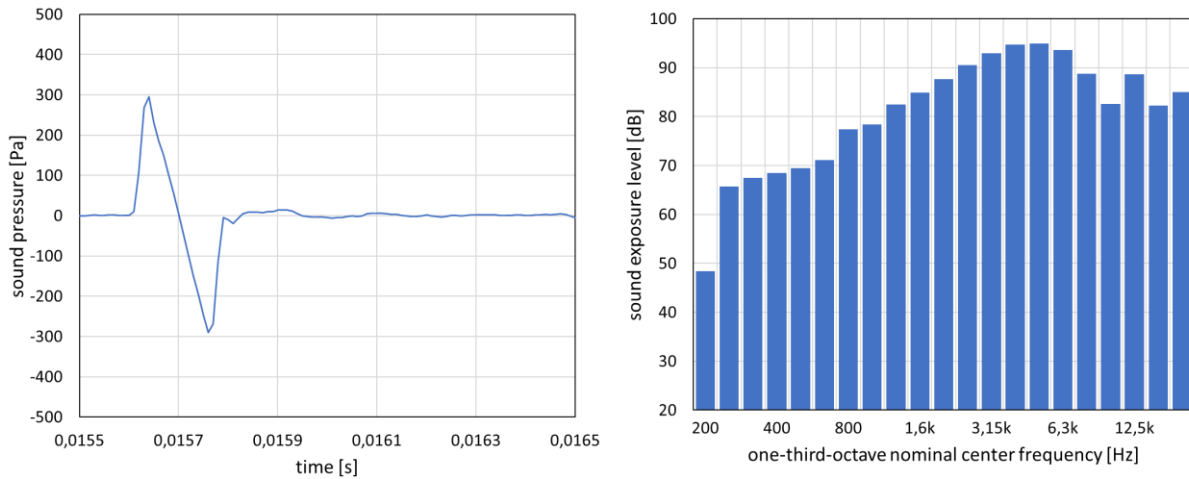


Figure 28 High resolution time history and relevant one-third-octave spectrum measuring circle 20 m at 10°, measuring height 2 m

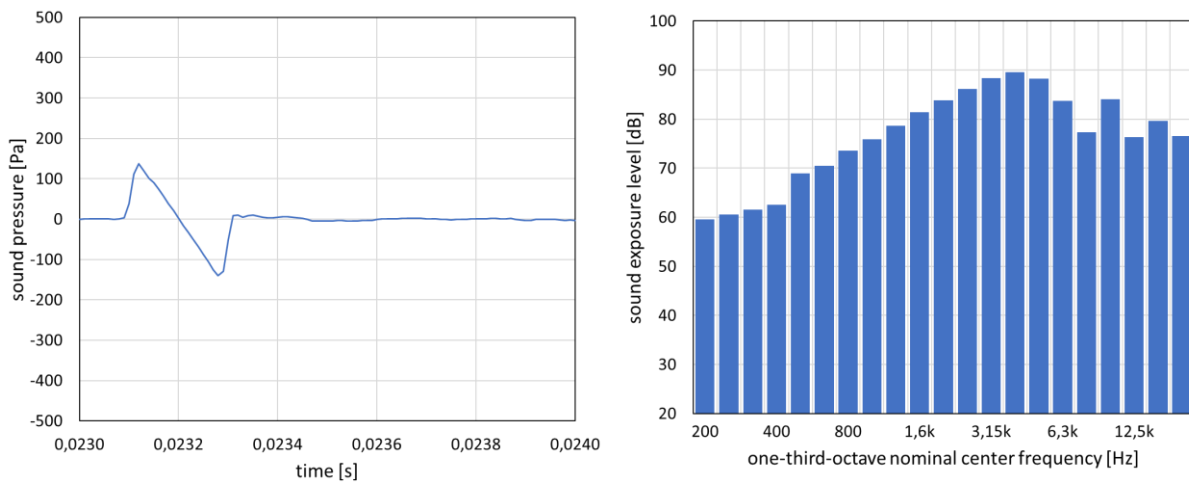


Figure 29 High resolution time history and relevant one-third-octave spectrum measuring circle 20 m at 30°, measuring height 2 m

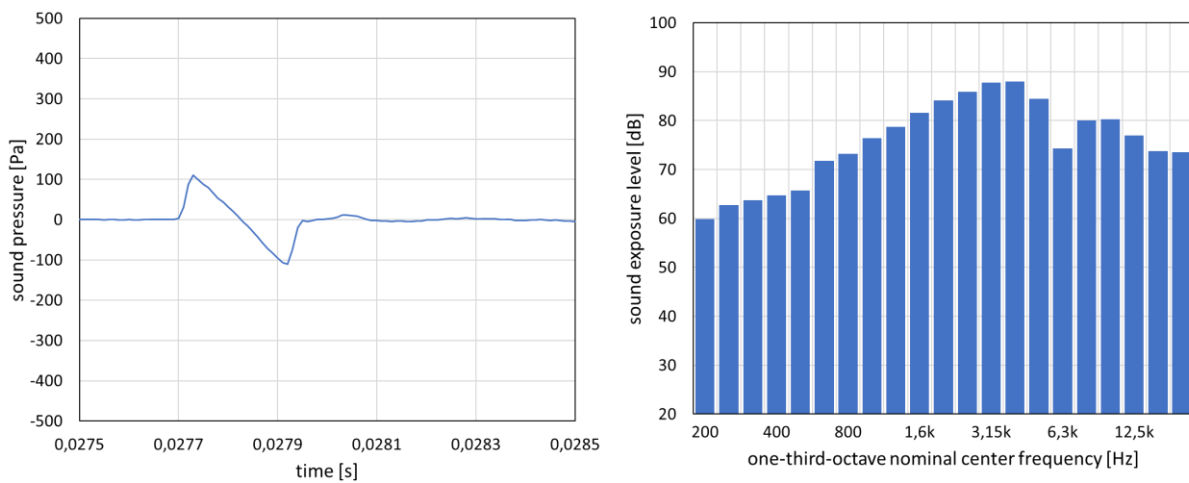


Figure 30 High resolution time history and relevant one-third-octave spectrum measuring circle 20 m at 50°, measuring height 2 m

Comparing the shape of theoretical spectrum of an N-wave, Figure 8, to the evaluated spectra gives some guidance on how to assess the reliability of the lower frequency bands.

The high-resolution time histories show the pure direct N-wave of the projectile sound. Please be aware, that the geometry is related to the muzzle. The real distance between the source point of the projectile sound to the receiver is rather small, see Figure 18.

All figures are scaled in the same way for comparison purposes. The time axis always indicates a window of 1 ms. The absolute time has no meaning in the given context. In all time histories the effect of the low sampling rate is obvious. Nevertheless, the time histories allow a reliable estimation of the duration and the peak pressure of the N-wave.

	1	2	3	4	5	6	7	8	9	10	11	12	13	14
1	quantity	Unit	caliber .223 Remington, flat shot											
2	angle	°	10	10	10	10	30	30	30	30	50	50	50	50
3	circle	m	10	10	20	20	10	10	20	20	10	10	20	20
4	height	m	1	2	1	2	1	2	1	2	1	2	1	2
5	L_{ZFmax}	dB	113,7	114,0	109,6	110,8	108,9	109,1	104,8	105,0	107,3	107,0	103,2	103,5
6	L_{ZSmax}	dB	104,6	105,0	100,5	101,8	99,9	100,0	95,7	96,0	98,2	98,0	94,2	94,5
7	L_{ZPeak}	dB	146,0	147,0	141,7	143,4	140,6	141,3	135,8	136,8	138,0	138,5	133,6	134,8
8	$L_{Zpeak,plus}$	dB	146,0	147,0	141,7	143,4	140,6	141,3	135,8	136,8	138,0	138,5	133,6	134,8
9	$L_{Zpeak,minus}$	dB	146,2	146,5	141,8	143,2	141,0	141,2	136,7	136,9	139,3	139,2	134,5	134,8
10	L_{EZ}	dB	104,6	105,0	100,5	101,8	99,9	100,0	95,7	96,0	98,2	98,0	94,2	94,5
11	L_{CFmax}	dB	113,2	113,5	109,2	110,3	108,6	108,7	104,4	104,6	107,0	106,6	103,0	103,3
12	L_{CSmax}	dB	104,2	104,4	100,2	101,3	99,5	99,6	95,4	95,6	98,0	97,6	94,0	94,2
13	L_{Cpeak}	dB	145,0	146,0	140,6	142,2	139,7	140,3	134,9	135,4	137,4	137,3	132,9	133,7
14	L_{EC}	dB	104,2	104,4	100,2	101,3	99,5	99,6	95,4	95,6	98,0	97,6	94,0	94,2
15	L_{AFmax}	dB	115,3	115,5	111,2	112,3	110,5	110,6	106,3	106,6	108,9	108,6	104,9	105,1
16	L_{ASmax}	dB	106,2	106,5	102,1	103,3	101,5	101,6	97,2	97,6	99,9	99,6	95,8	96,1
17	L_{Apeak}	dB	146,4	147,5	142,0	143,7	140,9	141,8	136,1	136,8	138,4	138,6	134,1	134,8
18	L_{EA}	dB	106,2	106,5	102,1	103,3	101,5	101,6	97,2	97,6	99,9	99,6	95,8	96,1
19	$E_{Z,s}$	Pa ² s	11,6	12,5	4,5	6,0	3,9	4,0	1,5	1,6	2,7	2,5	1,1	1,1
20	$E_{C,s}$	Pa ² s	8,3	8,5	3,4	4,3	3,0	3,0	1,2	1,2	2,1	1,9	0,9	0,9
21	$E_{A,s}$	Pa ² s	12,4	12,7	5,0	6,4	4,4	4,4	1,7	1,8	3,1	2,8	1,3	1,3
22	$L_{EZ,s}$	dB	104,6	104,9	100,5	101,7	99,9	100,0	95,7	96,0	98,2	98,0	94,2	94,5
23	$L_{EC,s}$	dB	103,2	103,3	99,2	100,3	98,8	98,8	94,7	94,9	97,3	96,8	93,4	93,6
24	$L_{EA,s}$	dB	104,9	105,0	100,9	102,0	100,4	100,4	96,3	96,5	98,9	98,5	95,0	95,2

Table 3 Results for some acoustical quantities of the projectile sound

key	<i>L</i>	level
	<i>Z, C, A</i>	acoustical frequency weighting
	<i>F, S</i>	acoustical time weighting
	<i>s</i>	values derived from the frequency domain
	<i>E</i>	exposure
	<i>max</i>	maximum value of the relevant time history
	<i>peakplus</i>	highest positive value of the relevant time history
	<i>peakplus</i>	highest positive value of the relevant time history

Table 3 compiles the available acoustical quantities calculated for time gate used to evaluate the one-third octave spectrum. These quantities are mostly evaluated in the time domain. The index s in Table 3 indicates, if the quantity uses the frequency domain (and the related time gate).

The give time histories and the spectra are rather reliable because they in not disturbed by any reflections or other signals. They can serve as a basis for model validation.

The reader may find the data for a .223 Remington shot on the internet, for example at [11]. The following analysis assumes the muzzle speed of the projectile to be 950 m/s, a (true) length of 0,028 m, an effective length of 0,024 m, a speed reduction per meter along the trajectory of 1,4 1/m, a drag coefficient of 0,25 and a projectile mass of 9,7 g

	1	2	3	4
1	Symbol	Reference	Unit	Value
3	v	projectile speed	m/s	950
4	m	projectile mass	kg	0,0097
6	d	projectile diameter	m	0,00565
7	l	projectile length l_{WHITHAM}	m	0,028
8	l_{eff}	projectile length l_{ISO17201}	m	0,025
9	A	projectile area	m ²	0,00004865
10	θ_e	Eq. 2 at segment end	°	68,866
11	θ_b	Eq. 2 at segment begin	°	69,029
12	$s_0 \equiv r_0$	Length unit, length of segment	m	1
13	M_b	MACH number at segment begin	1	2,7941
14	M_e	MACH number at segment end	1	2,7735
15	C_w	drag coefficient along segment	1	0,25
16	t_{clin}	Eq. 31	ms	0,215
17	f_{clin}	Eq. 32	Hz	4604
39	r_{lin}	Eq. 27	m	21,4
18	Q	Eq. 4	J	6,5640
19	Q	Eq. 5	J	6,5640
20	ΔE_{kin}	Loss of kinetic energy	J	12,9
23	σ_{ac}	acoustical efficiency	%	10
30	$\kappa_{\text{ISO17201-4}}$	Change of speed per one meter	1/s	-1,4
29	$L_{\text{Ep,bb,i}}$	Eq. 12 Part 4 exposure level	dB	110,06

Table 4 Some model results for .223 Remington shot signals

Table 4 gives some basic model results. These results describe the source. They hold for each receiver point.

1	2	3				4				5			
Measure	Unit	Value											
angle, Figure 18	°	10				30				50			
circle, Figure 18	m	10		20		10		20		10		20	
height, Figure 18	m	1	2	1	2	1	2	1	2	1	2	1	2
distance, Figure 18	m	2,1	1,8	3,7	3,8	5,3	5,3	10,6	10,6	8,1	8,1	16,3	16,3
$S_{cylinder}$	m ²	12,5	10,8	21,3	21,8	30,0	30,0	59,0	59,0	45,4	45,4	90,3	90,3
S_{Wedge}	m ²	0,0	0,0	0,1	0,1	0,1	0,1	0,4	0,4	0,2	0,2	0,9	0,9
E	Pa ² s	21,4	24,7	12,6	12,3	8,9	8,9	4,5	4,5	4,5	4,5	2,9	2,9
L_E	dB	107,3	107,9	105,0	104,9	103,5	103,5	100,5	100,5	101,7	101,7	98,7	98,7
p_{peak}	Pa	707	774	505	497	406	406	265	265	313	313	203	203
$p_{c,Whitham}$	Pa	570	640	373	365	285	285	169	169	207	207	123	123
$A_{nlin,ISO17201-4}$	dB	0,81	0,64	1,42	1,45	1,81	1,81	2,56	2,65	2,27	2,27	3,03	3,03
$L_{E,ISO17201-4}$	dB	106,0	106,9	102,9	102,8	100,9	100,9	97,1	97,1	98,6	98,6	94,7	94,7
$p_{peak,ISO17201-4}$	Pa	610,6	685,7	398,4	390,4	303,6	303,6	179,2	179,2	220,0	220,0	128,8	128,8
$L_{p,peak,ISO17201-4}$	dB	147,9	150,7	146,0	145,8	143,6	143,6	139,0	139,0	140,8	140,8	136,2	136,2
$f_{c,ISO17201-4}$	Hz	7785	8090	6757	6712	6176	6176	5194	5194	5555	5555	4664	4664
$t_{c,ISO17201-4}$	ms	0,129	0,124	0,148	0,149	0,162	0,162	0,193	0,193	0,180	0,180	0,214	0,214
$t_{c,measured}$	ms	0,20	0,18	0,19	0,2	0,21	0,21	0,26	0,23	0,23	0,22	0,25	0,26
$f_{c,measured}$	Hz	4975	5556	5263	5000	4762	4762	3846	4349	4349	4545	4000	3846
$L_{E,measured}$	dB	104,6	105,0	100,5	101,8	99,9	100,0	95,7	96,0	98,2	98,0	94,2	94,5
$L_{p,peak,measured}$	dB	146,0	147,0	141,7	143,4	140,6	141,3	135,8	136,8	138,0	138,5	133,6	134,8
$p_{peak,measured}$	Pa	400	448	243	296	215	232	123	138	159	168	98	110

Table 5 Comparison of model predictions to measured values

Table 5 compares the receiver dependent model results to the measured values. The author leaves it to the reader to draw some conclusion.

9 Conclusion

As a part of the series of essay called ‘bella acoustica – bellum acousticum’ this essay is not intended to be a scientific report or review on projectile sound covering all the physical and acoustical aspect of the topic. It just collects some information and let the reader be part of the challenge to understand, predict and measure projectile sound.

Projectile sound is not a simple superposition of spherical waves radiated from moving point source along the trajectory. Projectile sound is generated through a complex process while a body is flying with supersonic speed. Therefore, this essay firstly tried to give some basic idea what projectile sound is about. The essay also discusses some models that can be used in acoustics to predict the sound exposure of projectile sound for noise assessment purposes.

The prediction of receiver levels of the projectile sound is a rather challenge for the following reasons:

- The application of the models to calculate source exposure levels needs a lot of information about the trajectory, the projectile (size and shape, drag coefficient) and so on that is not available in most cases.
- In a significant large region, projectile sound propagates non-linear due the high levels and the signal shape. Non-linearity adds a lot of uncertainties to all engineering models.
- If shooting ranges with side berms and safety baffles are involved, the prediction of shielding attenuation is most important. Due to the non-linear change of the shape of the signal and due to the strong directionality of this sound models to estimate the shielding effect will basically fail.
- Predicting relevant receiver levels needs a reliable modelling of the ground reflection(s). At relevant receiver point projectile sound and its ground reflections arrive at grazing incident which can strongly influence the receiver levels. Therefore, the analysis of receiver signals is rather complex.

10 References

- [1] Zangers, J.; Hirsch, K.-W.: "Zur Berechnung des Geschosknalls von Flugkörpern auf ballistischen Flugbahnen", Fortschritte der Akustik, DAGA'2008, DEGA e.V., Dresden
- [2] Zangers, J: Private Communication on the integration of the drag-force along a segment of a projectile trajectory, 2008, unpublished background paper to [1]
- [3] Lapua Bullets Drag Coefficients: <http://www.lapua.com/upload/ballistics/qtu-lapua-edition-2010.pdf>, visited 2018-07-11.
- [4] DIN EN ISO 17201-4, "Acoustics — Noise from shooting ranges — Part 4: Prediction of projectile sound.
- [5] Witham, G.B.: „The behaviour of a supersonic flow past a body of revolution far from the axis“, *Proc. R. Soc. London*, Ser A261(1950) pp. 89-109 1950
- [6] Witham G.B.: „The flow pattern of a supersonic projectile“, *Commun. Pure Apl. Math.* V (1952) pp.301-348
- [7] McCoy R. L.: "Modern Exterior Ballistics – The Launch and Flight Dynamics of Symmetric Projectiles", Schiffer Publishing Ltd, 2nd edition, 2012
- [8] Buchta, E.; Hirsch, K.-W.: "Low-frequency projectile noise from flat howitzer shots", Proceedings Internoise '2000, Nice
- [9] Hirsch, K.-W.; Buchta, E.: "Analysis of low-frequency projectile noise signals measured close to the ground", Proceedings Internoise '2000, Nice
- [10] Hirsch, K.-W., Bertels, W.: "Estimation Of The Directivity Pattern Of Muzzle Blasts", Fortschritte der Akustik, AIA-DAGA'2013, DEGA e.V., Meran
- [11] Projectile data .223 Remington:
https://de.wikipedia.org/wiki/5,56_%C3%97_45_mm_NATO, visited 2018-08-16

11 Appendix

11.1 Remark on Eq. 28

$$\begin{aligned}
 t_{clin} &= \frac{1}{f_0} \frac{M^{\frac{3}{4}}}{(M^2-1)^{\frac{1}{4}}} \frac{d_p}{l_p^{\frac{1}{4}}} \frac{1}{r_0} \left[\left(0,54 \frac{P_{atm}}{P_{lin}} \right)^{\frac{4}{3}} \sqrt[3]{\frac{d^4}{l} \frac{M^3}{(M^2-1)}} \right]^{\frac{1}{4}} \\
 &= \frac{1}{f_0} \left(0,54 \frac{P_{atm}}{P_{lin}} \right)^{\frac{1}{3}} \frac{M}{(M^2-1)^{\frac{1}{4}}} \frac{d_p}{l_p^{\frac{1}{4}}} \frac{1}{r_0} \left[\sqrt[3]{\frac{d^4}{l} \frac{1}{(M^2-1)}} \right]^{\frac{1}{4}} \\
 &= \frac{1}{f_0} \left(0,54 \frac{P_{atm}}{P_{lin}} \right)^{\frac{1}{3}} \frac{M}{(M^2-1)^{\frac{1}{4}}} \frac{d_p}{l_p^{\frac{1}{4}}} \frac{1}{r_0} \left(\frac{d^4}{l} \frac{1}{(M^2-1)} \right)^{\frac{1}{12}} \\
 &= \frac{1}{f_0 r_0} \left(0,54 \frac{P_{atm}}{P_{lin}} \right)^{\frac{1}{3}} \frac{M}{(M^2-1)^{\frac{1}{3}}} \frac{d_p}{l_p^{\frac{1}{4}}} \left(\frac{d^4}{l} \right)^{\frac{1}{12}} \\
 &= \frac{1}{f_0 r_0} \left(0,54 \frac{P_{atm}}{P_{lin}} \right)^{\frac{1}{3}} \frac{M}{(M^2-1)^{\frac{1}{3}}} \frac{d_p d^{\frac{1}{3}}}{l_p^{\frac{1}{4}} l^{\frac{1}{12}}} \\
 &= \frac{0,0467 \text{ s}}{r_0} \frac{M}{(M^2-1)^{\frac{1}{3}}} \frac{d_p d^{\frac{1}{3}}}{l_p^{\frac{1}{4}} l^{\frac{1}{12}}} \\
 &= \frac{d_p}{f_0 r_0} \sqrt[3]{0,54 \frac{P_{atm}}{P_{lin}} \frac{M^3}{(M^2-1)} \frac{d}{l}}
 \end{aligned}$$

11.2 Drag coefficient

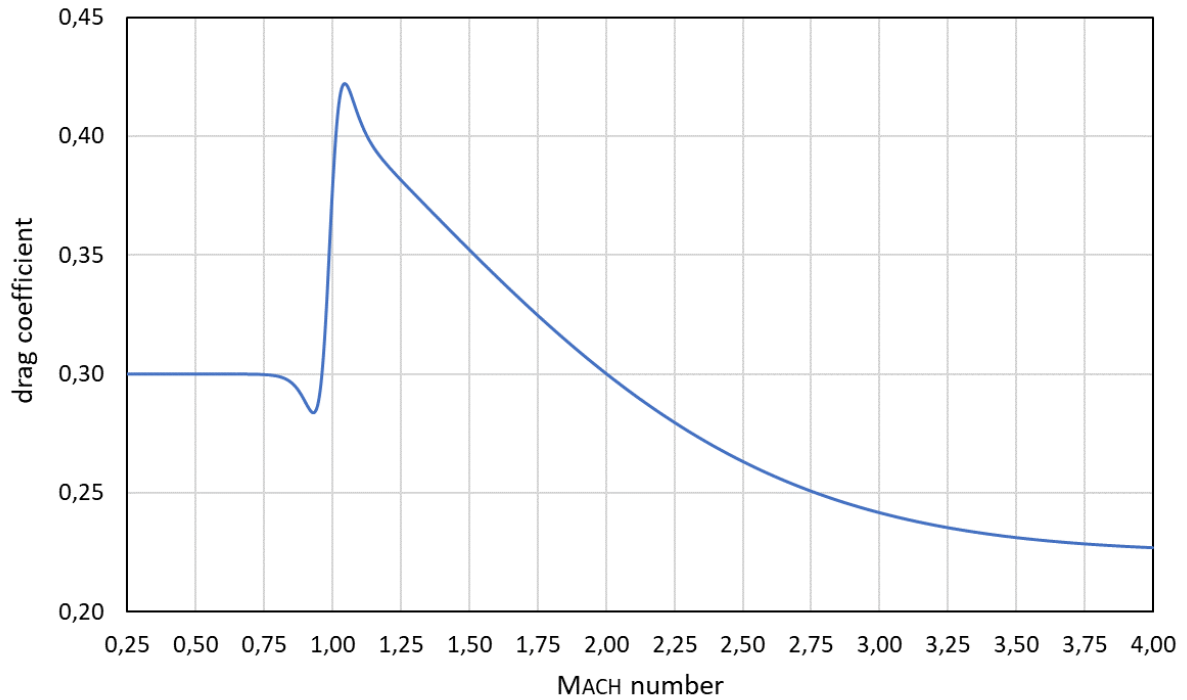


Figure 31 Measured drag coefficient of a projectile of a rifle, after [3]

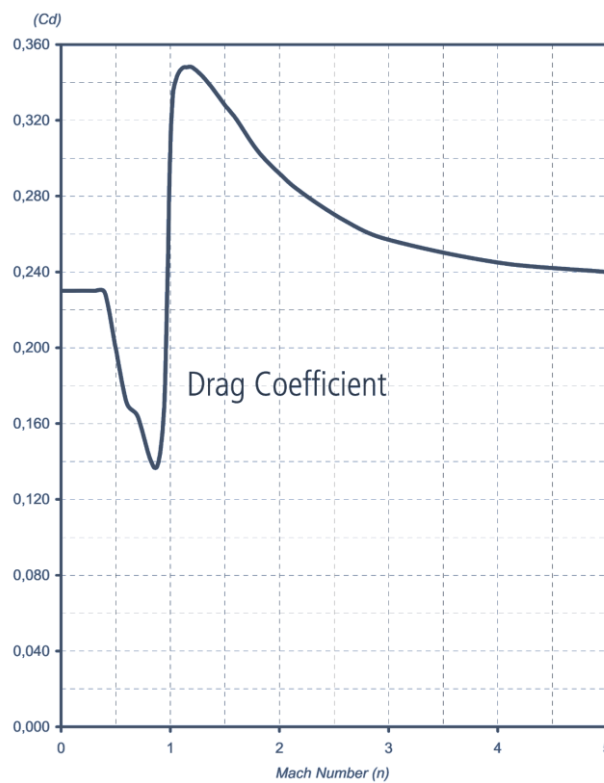


Figure 32 Measured drag coefficient of a projectile of a rifle, after [3]

Figure 31 indicates the drag coefficient of a .308 Winchester projectile. It was backward calculated using a dedicated program of the author to estimate trajectories of civil and military weapons. Figure 32 depicts a measured drag coefficient for a rifle.

Though both figures show significant differences, the general behavior of the drag coefficient of a streamlined projectile is clear. The drag coefficient has a steep rise that begins just before the speed of sound and ends just behind that critical speed. At larger speeds the drag coefficient decreases exponentially.

Therefore, for the prediction of projectile sound from projectiles in the vicinity of the speed of sound it is strongly recommended to use Eq. 3 to estimate the source energy.

11.3 Trajectory

The following figures provide some insight into a typical trajectory of a rifle shot.

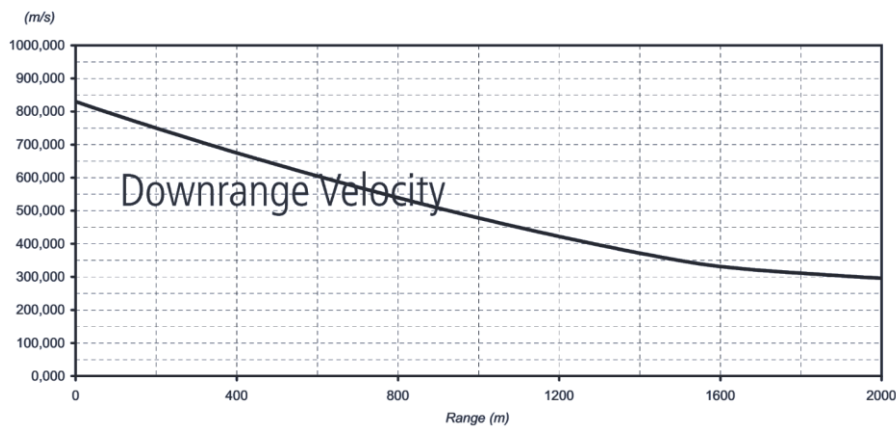


Figure 33 Speed of the projectile versus distance, after [3]

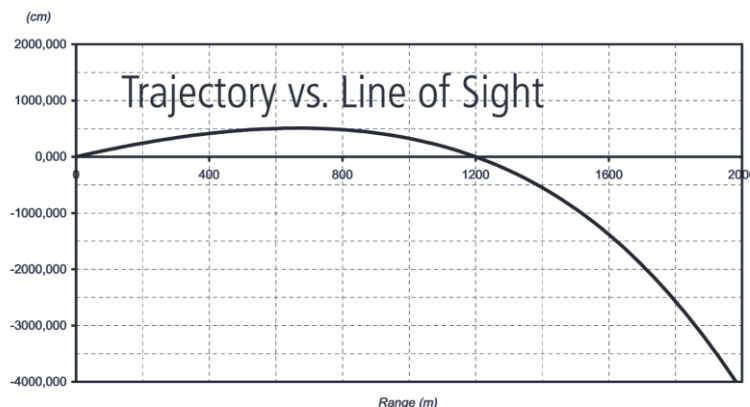


Figure 34 Height of projectile versus distance, after [3]

12 Über „Bella Acustica – De Bello Acustico“



**Eine Sammlung von Aufsätzen
 zu ausgewählten Themen der Akustik
 aus der ganz persönlichen Sicht des Autors**

	Prolog Die Schöne und der Krieg	kwhdba.00.01 2018-10-03	E
	Dezibels Warum sich Akustiker in der Wüste am wohlsten fühlen	kwhdba.01.01 2018-10-07	E
	Bewertungen Wie die Ohren hören sollten	kwhdba.02.01 2016-11-09	E
	Zeit begreifen Zeitbegriffe	kwhdba.03.00 2016-11-12	F
	Rote Rosen Prognosen mit dem Schallwetter	kwhdba.04.00 2016-11-12	I
	Pegelsalat Zur systematischen Kennzeichnung von Schallpegeln	kwhdba.05.00 2016-11-12	F
	Vom Harten und Weichen Bodenreflexionen im Freien	kwhdba.06.00 2016-11-12	I
	Atmosphärische Störungen Über Messungen im Freien	kwhdba.07.00 2016-11-21	F
	Projectile Sound To Whom It May Concern	kwhdba.08.01 2018-08-22	E
	Überreichweiten Über Zonen abnormaler Hörbarkeit	kwhdba.09.1 2018-09-17	E
	Götzenverehrung DIN ISO 9613	kwhdba.10.0 2018-10-06	K

Stand	I	Idee	erste Skizze	---	E	Entwurf	kurz vor druckreif	web
	F	Fragmente	erste Abschnitte oder Kapitel	---	D	Druck	Druckversion	web
	K	Konzept	Konzept ohne Sprachprüfung	web				

Impressum

Autor
Urheberrecht
Zitierhinweis
Verfügbarkeit
Kontakt



Karl-Wilhelm Hirsch
<https://creativecommons.org/licenses/by/4.0/deed.de>
Hirsch, K.-W.: „Bella Acustica – De Bello Acustica“, [Titel], [Kennung]
www.kwhirsch.de
post@kwhirsch.de